Table 1. Density of neurons in motor nerve nuclei and spinal cord

Nucleus	Control ($n = 3$) neurons/mm^3	AR2 ($n = 4$) neurons/mm^3
III	11,253 ± 1783	10,441 ± 632
IV	15,783 ± 1694	16,032 ± 658
VI	10,117 ± 996	10,699 ± 195
Vm	8809 ± 417	8623 ± 246
Vm (>25 μm)	3603 ± 213	2767 ± 175**
VII	1041 ± 124	1016 ± 96
VII (>20 μm)	91.1 ± 32.7	67.7 ± 13.1**
X	11,442 ± 1932	11,652 ± 2387
XII	11,800 ± 541	9834 ± 1530
XII (>20 μm)	832.7 ± 92.9	677.8 ± 116.2**
C5 AH (≤20 μm)	37,147 ± 326	37,941 ± 331
C5 AH (>20 μm)	25.5 ± 0.9[a]	13.7 ± 0.7[a,**]
L5 AH (>20 μm)	29.3 ± 0.32[a]	15.9 ± 0.31[a,**]
DH	476,312 ± 12,623	498,816 ± 21,446
VR	840.0 ± 26.5[b]	626.3 ± 31.4[b,*]

Numbers are the neuronal density per cubic millimeter (mean ± SEM) in each nucleus from mice at 12 months of age. For Vm, VII, and XII, neurons with large diameter (>20 or 25 μm) were also counted. AR2, *ADAR2*$^{flox/flox}$/VAChT–Cre.Fast mice; III, nucleus of oculomotor nerve; IV, nucleus of trochlear nerve; VI, nucleus of abducens nerve; Vm, motor nucleus of trigeminal nerve; VII, nucleus of facial nerve; X, dorsal nucleus of the vagus nerve; XII, nucleus of hypoglossal nerve; C5 AH, anterior horn of the fifth cervical cord; L5 AH, anterior horn of the fifth lumbar cord; DH, zona gelatinosa of the spinal cord; VR, ventral roots (L5). *$p < 0.005$; **$p < 0.001$ (ANOVA).

[a]Number of neurons per section.

[b]Number of axons.

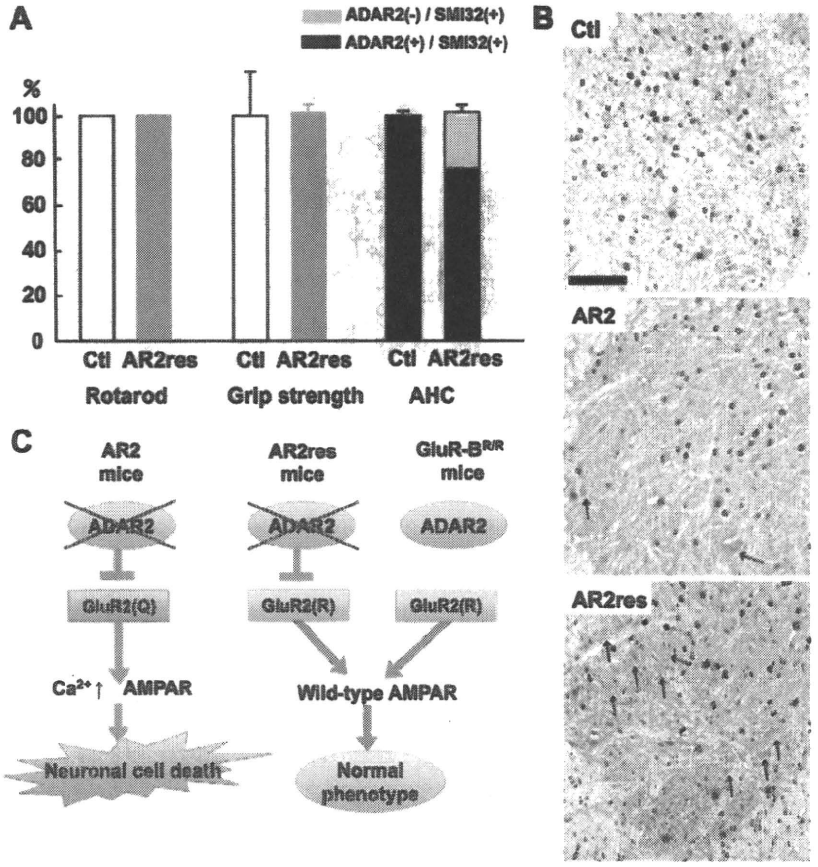

Figure 5. Crucial role of GluR2 Q/R site editing in death of ADAR2-deficient motor neurons. ***A***, AR2/GluR-$B^{R/R}$ mice (AR2res) displayed full rotarod score and normal grip strength at 6 months of age compared with control mice (Ctl). The number of total AHCs, of which a considerable proportion was deficient in ADAR2, did not decrease in AR2res mice. ***B***, At 6 months of age, although only a few AHCs lacking ADAR2 immunoreactivity (arrowheads) were observed in AR2 mice, a considerable number of AHCs lacking ADAR2 immunoreactivity was present in AR2res mice. The density of AHCs in AR2res mice was similar to that in the control mice in which all the AHCs were immunoreactive to ADAR2 in their nuclei. Sections were counterstained with hematoxylin. Scale bar, 100 μm. ***C***, Scheme illustrating that lack of ADAR2 induces slow death of motor neurons in AR2 mice but not in AR2res mice that express Q/R site-edited GluR2 in the absence of ADAR2 activity. The exonic Q codon at the Q/R site of GluR2 was substituted by an R codon in the endogenous GluR2 alleles of GluR-$B^{R/R}$ mice.

AR2/GluR-$B^{R/R}$ mice (AR2rescue, or AR2res, mice) were phenotypically normal and had full motor function until 6 months of age (Fig. 5*A*). The AHCs, including the ~30% AHCs lacking ADAR2 from Cre-mediated recombination, were viable in AR2res mice at 6 months of age, and the total number of AHCs was the same as in age-matched control mice (Fig. 5*A*,*B*). Consistent with a lack of AHC loss, there was no detectable increase in GFAP or MAC2 immunoreactivity in the anterior horns (supplemental Fig. S2*C*, available at www.jneurosci.org as supplemental material). These results demonstrate that it is specifically the failure of GluR2 Q/R site editing by which ADAR2 deficiency induces the slow death of motor neurons (Fig. 5*C*).

Discussion

We generated the AR2 mouse (Hideyama et al, 2008), a conditional ADAR2 knock-out line, which carries gene-targeted floxed ADAR2 alleles that become functionally ablated by Cre recombinase expressed from a transgene (VAChT–Cre.Fast) in ~50% of motor neurons (Misawa et al., 2003). These displayed progressive motor dysfunctions. The ADAR2-lacking motor neurons expressed only Q/R site-unedited GluR2. Virtually all of the ADAR2-lacking AHCs underwent degeneration, whereas the surviving ADAR2-expressing AHCs remained intact by 12 months of age. The death of ADAR2-lacking AHCs was completely prevented by a point mutation in the endogenous GluR2 alleles of AR2 mice, thus generating Q/R site-edited GluR2 in the absence of ADAR2 (Kask et al., 1998). These findings highlight the crucial role of RNA editing at the GluR2 Q/R site for survival of motor neurons and demonstrate that expression of Q/R site-unedited GluR2 is a cause of slow death of motor neurons. Therefore, it is necessary to investigate the relevance of inefficient GluR2 Q/R site-RNA editing found in the patient's motor neurons to the pathogenesis of sporadic ALS (Kawahara et al., 2004; Kwak and Kawahara, 2005).

Concomitant with the loss of ADAR2-lacking AHCs, proximal and distal axons of AHCs underwent degeneration with resultant neurogenic changes in neuromuscular units. These pathological changes in AHCs and neuromuscular units caused motor dysfunctions in AR2 mice. The prevention of slow neuronal cell death observed in AR2 mice by GluR-B^R alleles expressing Q/R site-edited GluR2 in the absence of ADAR2 (Kask et al., 1998) means that, although ADAR2 edits numerous A-to-I positions in many RNAs expressed in the mammalian brain (Levanon et al., 2004; Li et al., 2009), failure of A-to-I conversions at sites other than the GluR2 Q/R site did not play a role in neuronal cell death (Fig. 5*C*).

When the GluR2 Q/R site is unedited, the Ca^{2+} permeability of the AMPA receptor is greatly increased, and trafficking of the receptor to synaptic membranes is facilitated (Sommer et al., 1991; Burna-

shev et al., 1992; Greger et al., 2002). This enhances neuronal excitability by increasing the density of Ca^{2+}-permeable functional AMPA channels, which is typically observed as fatal epilepsy in mice carrying Q/R site-uneditable GluR-*B* (*GluR2*) alleles (Brusa et al., 1995; Feldmeyer et al., 1999) and in systemic ADAR2-null mice (Higuchi et al., 2000). The results obtained from AR2 mice indicate that motor neurons expressing only Q/R site-unedited GluR2 undergo slow death when the mice live sufficiently long.

Some ADAR2-lacking AHCs die shortly after recombination, whereas others survive for more than 1 year. These observations indicate that, although all the ADAR2-lacking AHCs undergo neuronal death, the ability to compensate for the increased Ca^{2+} overload through the functionally altered AMPA receptor differs among AHCs. It is likely that the increased Ca^{2+} overload might have already led to dysfunction of the ADAR2-lacking AHCs before their death, causing a decline of motor functions at earlier stages. Vulnerability of motor neurons to Ca^{2+}-permeable AMPA receptor-mediated toxicity was demonstrated in GluR-B(N) transgenic mice, which additionally to wild-type GluR2 express an engineered GluR2 subunit that features asparagine (N) in place of glutamine (Q) at the Q/R site (Kuner et al., 2005). ADAR2 activity is downregulated in the rat after transient forebrain ischemia, resulting in the selective death of hippocampal CA1 pyramidal cells (Peng et al., 2006).

An intriguing observation in AR2 mice was the selective vulnerability among motor neurons in different cranial nerve nuclei. Neurons in facial and hypoglossal nerve nuclei decreased in number, whereas those in the oculomotor nerve nuclei did not, although the extent of GluR2 Q/R site editing was significantly reduced in all these nuclei. These results indicate that motor neurons in the oculomotor nerve nuclei can survive despite the incomplete nature of GluR2 Q/R site editing. Notably, motor neurons in the nuclei of oculomotor nerves are also much less vulnerable in ALS patients; this has been attributed to differential expression levels of Ca^{2+}-binding proteins, particularly parvalbumin, among motor neurons in different cranial nerve nuclei. Expression of parvalbumin is high in oculomotor neurons and low in the facial and spinal motor neurons (Ince et al., 1993). Indeed, overexpression of parvalbumin attenuated kainate-induced Ca^{2+} transients and protected spinal motor neurons from resultant neurotoxicity in parvalbumin transgenic mice (Van Den Bosch et al., 2002). It is likely that neurons with an efficient Ca^{2+}-buffering system, such as oculomotor neurons, are resistant to Ca^{2+} overload resulting from Ca^{2+}-permeable AMPA receptors.

The present results indicate that the failure of A-to-I conversion at the Q/R site of GluR2 pre-mRNA in motor neurons of sporadic ALS patients (Takuma et al., 1999; Kawahara et al., 2004; Kwak and Kawahara, 2005) is likely attributable to reduced ADAR2 activity. Indeed, the expression level of ADAR2 mRNA was decreased in the spinal cord of patients with sporadic ALS (Kawahara and Kwak, 2005). Molecular abnormalities found in postmortem tissues of patients with neurodegenerative diseases have shown signs of mechanisms underlying the disease and may represent both the neuronal death process and death-protective reactions arising from the protracted nature of the death process. It is therefore necessary to determine whether these molecular abnormalities are the cause or the result of neuronal cell death by developing an appropriate animal model. Although excitotoxicity has long been implicated in the pathogenesis of neurological diseases including ALS (Vosler et al., 2008; Bezprozvanny, 2009), surprisingly little direct evidence indicating excitotoxic neuronal cell death has been demonstrated in patient-derived materials. Here we demonstrate that the molecular abnormality found in motor neurons of patients with sporadic ALS is a direct cause of neuronal death in mice via a mechanism upregulating Ca^{2+}-permeable AMPA receptors. In addition, the AR2 mice possess certain characteristics found in ALS, including slow progressive death of motor neurons, neuromuscular unit-dependent motor dysfunction and differential low vulnerability of motor neurons of extraocular muscles. Therefore, this mouse model mimicking patient-derived molecular abnormalities may be useful for research on sporadic ALS.

References

Akbarian S, Smith MA, Jones EG (1995) Editing for an AMPA receptor subunit RNA in prefrontal cortex and striatum in Alzheimer's disease, Huntington's disease and schizophrenia. Brain Res 699:297–304.

Beleza-Meireles A, Al-Chalabi A (2009) Genetic studies of amyotrophic lateral sclerosis: controversies and perspectives. Amyotroph Lateral Scler 10:1–14.

Bezprozvanny I (2009) Calcium signaling and neurodegenerative diseases. Trends Mol Med 15:89–100.

Brusa R, Zimmermann F, Koh DS, Feldmeyer D, Gass P, Seeburg PH, Sprengel R (1995) Early-onset epilepsy and postnatal lethality associated with an editing-deficient GluR-B allele in mice. Science 270:1677–1680.

Burnashev N, Monyer H, Seeburg PH, Sakmann B (1992) Divalent ion permeability of AMPA receptor channels is dominated by the edited form of a single subunit. Neuron 8:189–198.

Carriedo SG, Yin HZ, Weiss JH (1996) Motor neurons are selectively vulnerable to AMPA/kainate receptor mediated injury *in vitro*. J Neurosci 16:4069–4079.

Feldmeyer D, Kask K, Brusa R, Kornau HC, Kolhekar R, Rozov A, Burnashev N, Jensen V, Hvalby O, Sprengel R, Seeburg PH (1999) Neurological dysfunctions in mice expressing different levels of the Q/R site-unedited AMPAR subunit GluR-B. Nat Neurosci 2:57–64.

Feng Y, Sansam CL, Singh M, Emeson RB (2006) Altered RNA editing in mice lacking ADAR2 autoregulation. Mol Cell Biol 26:480–488.

Greger IH, Khatri L, Ziff EB (2002) RNA editing at arg607 controls AMPA receptor exit from the endoplasmic reticulum. Neuron 34:759–772.

Greger IH, Khatri L, Kong X, Ziff EB (2003) AMPA receptor tetramerization is mediated by Q/R editing. Neuron 40:763–774.

Hideyama T, Yamashita T, Tsuji S, Misawa H, Takahashi R, Suzuki T, Kwak S (2008) Slow neuronal death of motor neurons in sporadic ALS mouse model by RNA editing enzyme ADAR2 knockout. Soc Abstr Neurosci 34:745.17.

Higuchi M, Maas S, Single FN, Hartner J, Rozov A, Burnashev N, Feldmeyer D, Sprengel R, Seeburg PH (2000) Point mutation in an AMPA receptor gene rescues lethality in mice deficient in the RNA-editing enzyme ADAR2. Nature 406:78–81.

Ince P, Stout N, Shaw P, Slade J, Hunziker W, Heizmann CW, Baimbridge KG (1993) Parvalbumin and calbindin D-28k in the human motor system and in motor neuron disease. Neuropathol Appl Neurobiol 19:291–299.

Kask K, Zamanillo D, Rozov A, Burnashev N, Sprengel R, Seeburg PH (1998) The AMPA receptor subunit GluR-B in its Q/R site-unedited form is not essential for brain development and function. Proc Natl Acad Sci U S A 95:13777–13782.

Kawahara Y, Kwak S (2005) Excitotoxicity and ALS: what is unique about the AMPA receptors expressed on spinal motor neurons? Amyotroph Lateral Scler Other Motor Neuron Disord 6:131–144.

Kawahara Y, Ito K, Sun H, Kanazawa I, Kwak S (2003a) Low editing efficiency of GluR2 mRNA is associated with a low relative abundance of ADAR2 mRNA in white matter of normal human brain. Eur J Neurosci 18:23–33.

Kawahara Y, Kwak S, Sun H, Ito K, Hashida H, Aizawa H, Jeong SY, Kanazawa I (2003b) Human spinal motoneurons express low relative abundance of GluR2 mRNA: an implication for excitotoxicity in ALS. J Neurochem 85:680–689.

Kawahara Y, Ito K, Sun H, Aizawa H, Kanazawa I, Kwak S (2004) Glutamate receptors: RNA editing and death of motor neurons. Nature 427:801.

Kawahara Y, Sun H, Ito K, Hideyama T, Aoki M, Sobue G, Tsuji S, Kwak S (2006) Underediting of GluR2 mRNA, a neuronal death inducing mo-

lecular change in sporadic ALS, does not occur in motor neurons in ALS1 or SBMA. Neurosci Res 54:11–14.

Kuner R, Groom AJ, Bresink I, Kornau HC, Stefovska V, Müller G, Hartmann B, Tschauner K, Waibel S, Ludolph AC, Ikonomidou C, Seeburg PH, Turski L (2005) Late-onset motoneuron disease caused by a functionally modified AMPA receptor subunit. Proc Natl Acad Sci U S A 102: 5826–5831.

Kwak S, Kawahara Y (2005) Deficient RNA editing of GluR2 and neuronal death in amyotropic lateral sclerosis. J Mol Med 83:110–120.

Levanon EY, Eisenberg E, Yelin R, Nemzer S, Hallegger M, Shemesh R, Fligelman ZY, Shoshan A, Pollock SR, Sztybel D, Olshansky M, Rechavi G, Jantsch MF (2004) Systematic identification of abundant A-to-I editing sites in the human transcriptome. Nat Biotechnol 22:1001–1005.

Li JB, Levanon EY, Yoon JK, Aach J, Xie B, Leproust E, Zhang K, Gao Y, Church GM (2009) Genome-wide identification of human RNA editing sites by parallel DNA capturing and sequencing. Science 324:1210–1213.

Lowe JS, Leigh N (2002) Motor neuron disease (amyotrophic lateral sclerosis). In: The Greenfield's neuropathology (Love S, Louis DN, Ellison DW, eds), pp 372–383. Oxford: Oxford UP.

Melcher T, Maas S, Herb A, Sprengel R, Seeburg PH, Higuchi M (1996) A mammalian RNA editing enzyme. Nature 379:460–464.

Misawa H, Nakata K, Toda K, Matsuura J, Oda Y, Inoue H, Tateno M, Takahashi R (2003) VAChT–Cre.Fast and VAChT–Cre.Slow: postnatal expression of Cre recombinase in somatomotor neurons with different onset. Genesis 37:44–50.

Nishimoto Y, Yamashita T, Hideyama T, Tsuji S, Suzuki N, Kwak S (2008) Determination of editors at the novel A-to-I editing positions. Neurosci Res 61:201–206.

Ohmae S, Takemoto-Kimura S, Okamura M, Adachi-Morishima A, Nonaka M, Fuse T, Kida S, Tanji M, Furuyashiki T, Arakawa Y, Narumiya S, Okuno H, Bito H (2006) Molecular identification and characterization of a family of kinases with homology to Ca^{2+}/calmodulin-dependent protein kinases I/IV. J Biol Chem 281:20427–20439.

Paschen W, Hedreen JC, Ross CA (1994) RNA editing of the glutamate receptor subunits GluR2 and GluR6 in human brain tissue. J Neurochem 63:1596–1602.

Paxinos G, Franklin KBJ (2001) The mouse brain in stereotaxic coordinates. San Diego: Academic.

Peng PL, Zhong X, Tu W, Soundarapandian MM, Molner P, Zhu D, Lau L, Liu S, Liu F, Lu Y (2006) ADAR2-dependent RNA editing of AMPA receptor subunit GluR2 determines vulnerability of neurons in forebrain ischemia. Neuron 49:719–733.

Rothstein JD, Martin LJ, Kuncl RW (1992) Decreased glutamate transporter by the brain and spinal cord in amyotrophic lateral sclerosis. N Engl J Med 326:1464–1468.

Sansam CL, Wells KS, Emeson RB (2003) Modulation of RNA editing by functional nucleolar sequestration of ADAR2. Proc Natl Acad Sci U S A 100:14018–14023.

Schymick JC, Talbot K, Traynor BJ (2007) Genetics of sporadic amyotrophic lateral sclerosis. Hum Mol Genet 16 [Spec No 2]:R233–R242.

Seeburg PH (2002) A to I editing: new and old sites, functions and speculations. Neuron 35:17–20.

Sommer B, Köhler M, Sprengel R, Seeburg PH (1991) RNA editing in brain controls a determinant of ion flow in glutamate-gated channels. Cell 67:11–19.

Suzuki T, Tsuzuki K, Kameyama K, Kwak S (2003) Recent advances in the study of AMPA receptors. Nippon Yakurigaku Zasshi 122:515–526.

Takemoto-Kimura S, Ageta-Ishihara N, Nonaka M, Adachi-Morishima A, Mano T, Okamura M, Fujii H, Fuse T, Hoshino M, Suzuki S, Kojima M, Mishina M, Okuno H, Bito H (2007) Regulation of dendritogenesis via a lipid-raft-associated Ca^{2+}/calmodulin-dependent protein kinase CLICK-III/CaMKIgamma. Neuron 54:755–770.

Takuma H, Kwak S, Yoshizawa T, Kanazawa I (1999) Reduction of GluR2 RNA editing, a molecular change that increases calcium influx through AMPA receptors, selective in the spinal ventral gray of patients with amyotrophic lateral sclerosis. Ann Neurol 46:806–815.

Van Damme P, Braeken D, Callewaert G, Robberecht W, Van Den Bosch L (2005) GluR2 deficiency accelerates motor neuron degeneration in a mouse model of amyotrophic lateral sclerosis. J Neuropathol Exp Neurol 64:605–612.

Van Den Bosch L, Schwaller B, Vleminckx V, Meijers B, Stork S, Ruehlicke T, Van Houtte E, Klaassen H, Celio MR, Missiaen L, Robberecht W, Berchtold MW (2002) Protective effect of parvalbumin on excitotoxic motor neuron death. Exp Neurol 174:150–161.

Vosler PS, Brennan CS, Chen J (2008) Calpain-mediated signaling mechanisms in neuronal injury and neurodegeneration. Mol Neurobiol 38: 78–100.

Yang JH, Sklar P, Axel R, Maniatis T (1995) Editing of glutamate receptor subunit B pre-mRNA in vitro by site specific deamination of adenosine. Nature 374:77–81.

Cell

An Inhibitor of a Deubiquitinating Enzyme Regulates Ubiquitin Homeostasis

Yoko Kimura,[1,*] Hideki Yashiroda,[1,3] Tai Kudo,[1] Sumiko Koitabashi,[1] Shigeo Murata,[3] Akira Kakizuka,[2] and Keiji Tanaka[1]
[1]Laboratory of Frontier Science, Tokyo Metropolitan Institute of Medical Science, 2-1-6, Kamikitazawa, Setagaya, Tokyo 156-8506, Japan
[2]Laboratory of Functional Biology, Kyoto University Graduate School of Biostudies & Solution Oriented Research for Science and Technology (JST), Kyoto 606-8501, Japan
[3]Laboratory of Protein Metabolism, Graduate School of Pharmaceutical Sciences, The University of Tokyo, Tokyo 113-0033, Japan
*Correspondence: kimura-yk@igakuken.or.jp
DOI 10.1016/j.cell.2009.02.028

SUMMARY

The dynamic and reversible process of ubiquitin modification controls various cellular activities. Ubiquitin exists as monomers, unanchored chains, or protein-conjugated forms, but the regulation of these interconversions remains largely unknown. Here, we identified a protein designated Rfu1 (*r*egulator of *f*ree *u*biquitin chains 1), which regulates intracellular concentrations of monomeric ubiquitins and free ubiquitin chains in *Saccharomyces cerevisiae*. Rfu1 functions as an inhibitor of Doa4, a deubiquitinating enzyme. Rapid loss of free ubiquitin chains upon heat shock, a condition in which more proteins require ubiquitin conjugation, was mediated in part by Doa4 and Rfu1. Thus, regulation of ubiquitin homeostasis is controlled by a balance between a deubiquitinating enzyme and its inhibitor. We propose that free ubiquitin chains function as a ubiquitin reservoir that allows maintenance of monomeric ubiquitins at adequate levels under normal conditions and rapid supply for substrate conjugation under stress conditions.

INTRODUCTION

Ubiquitination is a reversible posttranslational modification of cellular proteins that plays important roles in the regulation of several cellular processes, such as protein quality control, protein trafficking, cell-cycle regulation, DNA repair, apoptosis, and signal transduction (Hershko and Ciechanover, 1998; Mukhopadhyay and Riezman, 2007). Ubiquitin (Ub) is a highly conserved 76 amino acid protein that covalently attaches to the lysine residue(s) of target proteins via its carboxy-terminal glycine residue. Since Ub itself contains seven lysines, it can attach to several other Ubs, allowing the formation of polyubiquitin chains. Thus, Ub exists intracellularly as either a monomer, a substrate-conjugated polyubiquitin or monoubiquitin, or unanchored Ub chains.

One of the well-characterized functions of Ub is serving as a tag for selective proteolysis by the 26S proteasome, which is a large multisubunit protease complex (Hershko and Ciechanover, 1998; Pickart and Eddins, 2004). In the ubiquitin-proteasome system (UPS), ubiquitination of a substrate is catalyzed by a Ub-activating enzyme (E1), a Ub-conjugating enzyme (E2), and a Ub-ligase (E3). Multiple Ubs are covalently added to a substrate successively by these enzymes, thus producing a substrate conjugated with polyubiquitin. The 26S proteasome recognizes the polyubiquitinated substrate and degrades the substrate after the polyubiquitin chain is cleaved off by deubiquitinating enzymes (DUBs) (Amerik and Hochstrasser, 2004; Ventii and Wilkinson, 2008). The released polyubiquitins or free Ub chains are further disassembled to monomeric Ubs by DUBs, and the resulting Ubs are reutilized.

Ubiquitination also plays a role in vacuolar sorting of both endocytic and biosynthetic membrane proteins (Mukhopadhyay and Riezman, 2007; Schnell and Hicke, 2003). At the endosome, Ub serves as a signal to sort cargo proteins into the multivesicular body (MVB), which is a critical step to their transport to lysosomes. Ub is removed from the cargo before entry into the internal vesicles of the MVB. In yeast, Doa4, a DUB, is responsible for deubiquitination of cargo proteins at the endosome (Katzmann et al., 2001; Nikko and Andre, 2007). Doa4 is recruited to the endosome and its activity is stimulated by Bro1, a class E Vps protein (Richter et al., 2007).

There seems to be a need for maintaining adequate intracellular levels of Ub, particularly the level of monomeric Ub, and indeed more Ubs are required under stress conditions (Finley et al., 1987). Yeast cells with insufficient amounts of monomeric Ub caused by mutation of DUB genes, such as *DOA4* or *UBP6*, are sensitive to an amino acid analog, and the expression of excess Ub compensates for this defect (Chernova et al., 2003; Papa and Hochstrasser, 1993; Swaminathan et al., 1999). Similarly, yeast cells become stress sensitive when *UBI4*, a heat shock gene encoding polyubiquitin, is deleted (Finley et al., 1987). In mice, a mutation in *Uch-L1* leads to gracile axonal dystrophy (*gad*) (Osaka et al., 2003). Moreover, the deletion of polyubiquitin gene *Ubc* and that of *Ubb* result in embryonic lethality and hypothalamic neurodegeneration, respectively (Ryu et al., 2007, 2008). However, an excess amount of Ub is also not beneficial to cells. In yeast, overexpression of Ub makes cells sensitive to stressful insults such as treatment with cadmium, arsenite, and paroromycin (Chen and Piper, 1995). To circumvent these situations, cells appear to possess several systems to regulate the level of monomeric Ub. One such regulatory system appears to operate at the level of transcription of

Ub-encoding genes. In yeast, among the four Ub-encoding genes *UBI1–4,* transcription of the *UBI4,* a polyubiquitin gene, is heat inducible (Finley et al., 1987). Another mechanism responsible for maintaining stable levels of intracellular Ub is an increase in Ubp6-associated proteasome in response to Ub deficiency, which efficiently retrieves Ub from Ub-conjugated substrate (Hanna et al., 2007).

Various eukaryotic organisms including mouse, rat, fly, nematoda, plants, and yeasts have significant intracellular levels of unanchored Ub chains, indicating the ubiquitous presence of such chains (van Nocker and Vierstra, 1993). However, the physiological significance of these chains remains largely elusive. The chains could be generated through release from polyubiquitinated substrates or by Ub-ligating enzymes from monomeric Ub. Several DUB mutants in yeast, including *doa4, ubp6, ubp8, ubp10,* and *ubp14*, show changes in monomeric Ub level and/or unanchored Ub chains or small Ub species (Amerik et al., 2000a). It was proposed that one function of unanchored Ub chains is competitive inhibition of polyubiquitin-substrate binding to the 26S proteasome (Amerik et al., 1997), but the exact roles of free Ub chains are poorly understood to date.

In the present study, we report the isolation of Rfu1. Rfu1 was found to regulate the cellular levels of monomeric Ub and free Ub chains and to inhibit Doa4. In addition, we found that heat shock rapidly and significantly decreased free Ub chains, and this effect was in part dependent on a balance between Doa4 and Rfu1. Based on our results, we propose that unanchored Ub chains serve as a Ub reservoir preventing the supply of excess amounts of monomeric Ubs under normal states but can supply monomeric Ubs rapidly when Ub is urgently required.

RESULTS

Isolation of Rfu1

To identify new cofactors of Cdc48, a protein involved in various cellular processes such as UPS-mediated protein degradation, membrane fusions, cell-cycle progression, and apoptosis (Woodman, 2003), we screened for multicopy suppressors of the *cdc48-3* temperature-sensitive mutant. In addition to *CDC48*-containing plasmids, we obtained several plasmids with an overlapping region (Figure 1A). Introduction of these plasmids suppressed the temperature-sensitive growth of *cdc48-3* at 34.5°C but not at 37°C, suggesting that their suppressing activities are partial. Deletion analysis identified the suppression activity in a fragment containing the entire YLR073c open reading frame (ORF) and its flanking regions (Figures 1A and 1B). We provisionally named this gene *RFU1* (regulator of free *u*biquitin chains 1, for the reason described below). *RFU1* encodes a protein of 200 amino acids and its function is unknown. Rfu1 displays marginal homology to two very different mammalian DUBs: AMSH and UBPY (alias UBP8) (Figure S1 available online) (McCullough et al., 2004; Naviglio et al., 1998; Row et al., 2007). The homologous regions are largely outside of the catalytic domain of these DUBs. Disruption of *RFU1* did not alter yeast cell growth at normal growth temperatures or at 37°C (Figures 1C and 1D), indicating that *RFU1* is a nonessential gene.

Genetic Interactions of *RFU1* with *cdc48-3* and Proteasome Genes

To examine whether Rfu1 and Cdc48 are involved in related functions, the *cdc48-3Δrfu1* double mutant was created. Indeed, we found that the *cdc48-3Δrfu1* mutant was more sensitive to elevated temperatures than the *cdc48-3* mutant (Figures 1C and 1D). In the next step, we examined the physical interaction between Cdc48 and Rfu1 by immunoprecipitation of 3×HA-tagged Rfu1, but we could not detect any apparent interaction (data not shown). These results suggest that *RFU1* is genetically related to *CDC48* but does not interact physically with Cdc48. Since one function of Cdc48 is to promote the degradation of proteins in the UPS (Ghislain et al., 1996), we examined whether UPS phenotypes would be enhanced by combining the *Δrfu1* mutation with a defect in the UPS machinery. We checked the temperature sensitivities of double mutants involving *Δrfu1* and two different proteasome mutants, *ΔN rpn2* and *rpt1/cim5-1.* Rpn2 and Rpt1 are a non-ATPase subunit and an ATPase subunit of the 26S proteasome, respectively (Ghislain et al., 1993; Isono et al., 2007). Both *Δrfu1ΔN rpn2* and *Δrfu1rpt1* mutants exhibited profound growth defects at elevated temperatures compared to *ΔN rpn2* and *rpt1* mutants, respectively (Figure 1E). The results led us to speculate that although Rfu1 may not be a Cdc48 cofactor, it appears to play an important role in the UPS in general. We therefore further investigated the function of Rfu1.

RFU1 Disruption and Overexpression Change Ub Profile

In spite of the genetic interactions of *RFU1* with various UPS genes, the degradation machinery in the UPS did not appear to be defective in the *Δrfu1* mutant. We examined the β-galactosidase activity of an exogenously expressed UFD (Ub fusion degradation) substrate, Ub-Pro-β gal (Figure S2) (Johnson et al., 1995). As expected, *cdc48-3* cells showed a significant increase of β-gal activity. In contrast, the *Δrfu1* mutant did not show a noticeable increase compared with the wild-type, indicating that Rfu1 is not involved in UPS-mediated protein degradation. In addition, we confirmed that *RFU1* deletion did not affect the mRNA levels of *UBI1–4* genes (Figure S3).

Since Rfu1 has a weak homology to two mammalian DUBs, and mutations of several yeast DUBs show characteristic changes in the bulk profile of cellular Ubs (Amerik et al., 2000a), we examined the Ub profiles of the *Δrfu1* mutant by using anti-Ub blot analysis. In our assay system, wild-type cells in early growth phase had a bulk Ub profile with monomeric Ub, unanchored Ub chains, as well as slowly migrated high-molecular-weight (HMW) forms, which presumably correspond to various Ub-conjugated proteins (Figure 2A). Surprisingly, the amount of free Ub chains was clearly decreased in *Δrfu1* cells, while the level of monomeric Ub was increased compared with the wild-type. In *cdc48-3* cells, HMW ubiquitinated proteins were increased and free Ub chains were decreased compared with wild-type cells. The *cdc48-3Δrfu1* cells showed further increase of HMW ubiquitinated protein levels relative to those of *cdc48-3* cells and marked reduction of free Ub chains (Figure 2A). Furthermore, cells carrying *Δrfu1ΔN rpn2* or *Δrfu1rpt1* mutations showed higher levels of HMW ubiquitinated proteins compared with cells harboring a single mutation of *ΔN rpn2* or *rpt1*, respectively

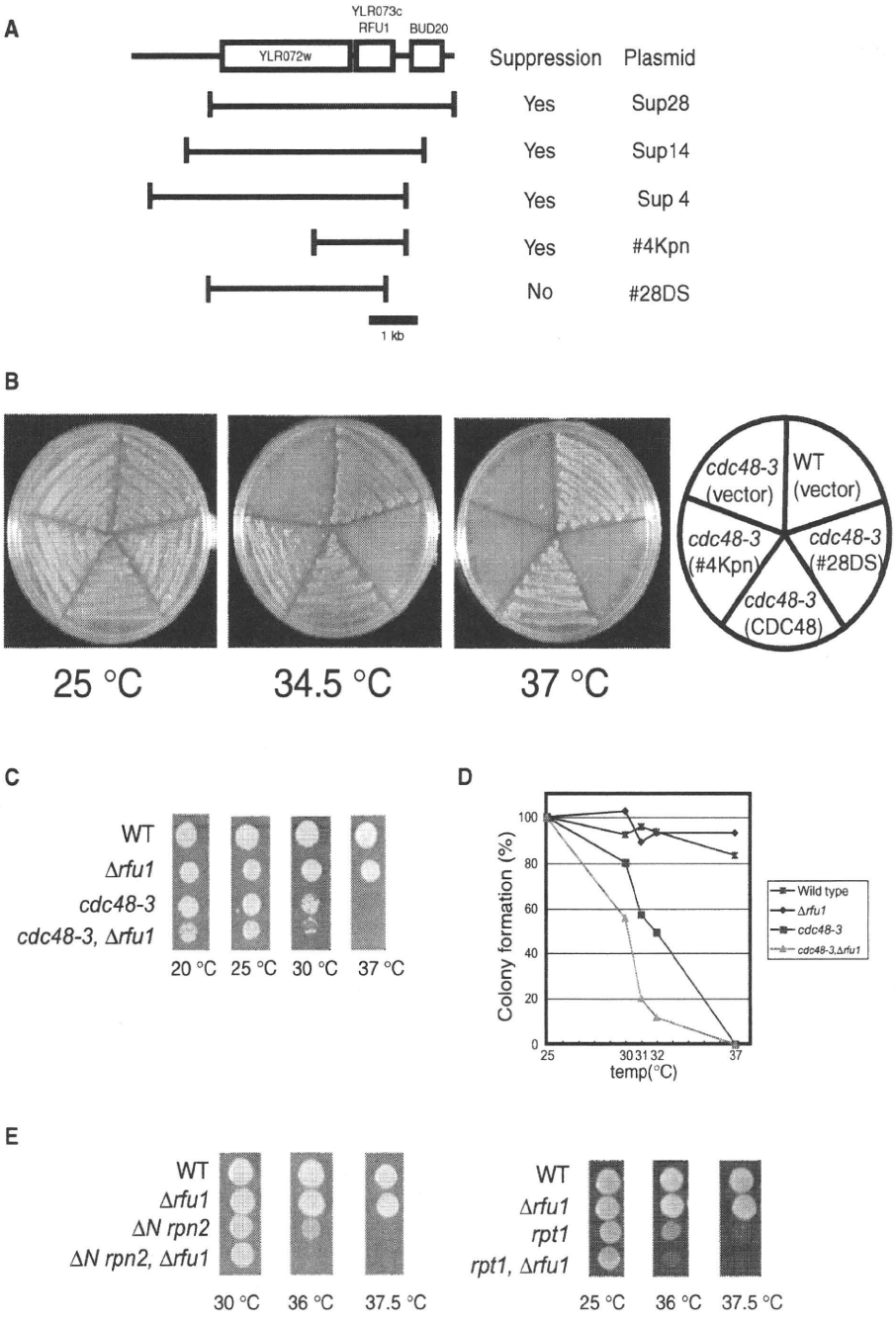

Figure 1. Isolation of *RFU1*

(A) DNA regions involved in suppressing the temperature-sensitive growth of *cdc48-3* and plasmids tested for their suppressor activity. Plasmid #28DS lacks the first 112 nucleotides of the *RFU1* gene.

(B) Effect of *RFU1* expression on the growth of *cdc48-3*. Wild-type cells with a vector, *cdc48-3* cells with a vector, and *cdc48-3* cells expressing the plasmid (*CDC48* or #4Kpn or #28DS) were streaked on SC-Trp plates and incubated at 25°C, 34.5°C, or 37°C for 3 days.

(C) Synthetic enhancements of growth sensitivity of *Δrfu1* with *cdc48-3*. Cells grown in early log phase were spotted on YPAD medium and grown at the indicated temperatures for 3 days.

(D) Colony-forming ability of wild-type, *Δrfu1*, *cdc48-3*, and *Δrfu1cdc48-3* cells at the indicated temperatures. Data are average of two experiments.

(E) Synthetic enhancements of growth sensitivity of *Δrfu1* with *ΔN rpn2* or *rpt1/cim5-1* mutation. Experiments were conducted as in (C).

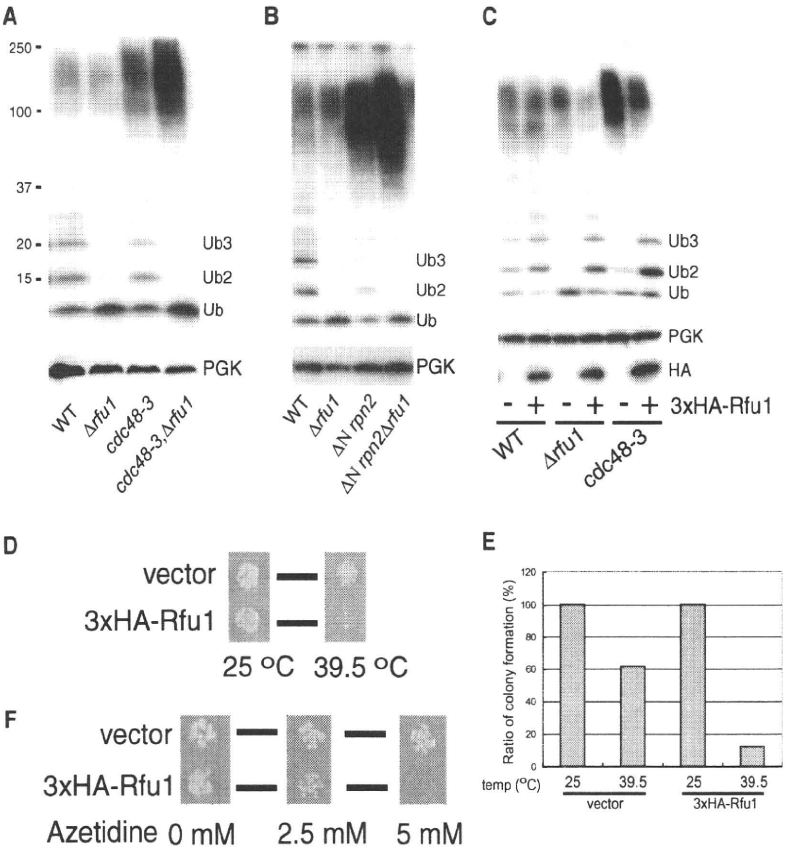

Figure 2. Changes in Accumulation of Different Ub Forms in *Δrfu1* and Other Mutants and Stress Sensitivity by Overexpression of Rfu1

(A) Disappearance of free Ub chains and high level of monomeric Ub in *Δrfu1* mutants. *Top*, anti-Ub immunoblot analysis. The position of size standard in kDa is indicated on the left. Monomeric Ub and Ub chain positions are marked. *Bottom*, anti-phosphoglycerate kinase (PGK) immunoblot, a control for protein loading.

(B) Accumulation of high-molecular-weight (HMW) ubiquitinated proteins in *ΔN rpn2Δrfu1* cells. Anti-Ub and anti-PGK immunoblot analyses were performed using wild-type, *Δrfu1*, *ΔN rpn2*, and *ΔN rpn2Δrfu1* cells.

(C) Effects of 3×HA-Rfu1 overexpression on Ub profiles. Immunoblot analyses using anti-Ub, anti-PGK, and anti-HA antibodies of wild-type, *Δrfu1*, or *cdc48-3* cells containing a vector or a plasmid that expresses 3×HA-Rfu1 under the GPD promoter.

(D) Sensitive phenotypes of 3×HA-Rfu1-overexpressing cells to sustained heat treatment. Wild-type cells containing a vector or a plasmid overexpressing 3×HA-Rfu1 were grown in early log phase at 25°C in SC-Ura culture. Cells were diluted and spotted on SC-Ura plates. Plates were placed at 39.5°C or 25°C for 17 hr and returned to 25°C, and viable cells were allowed to grow for 2 days.

(E) Quantitative analysis of (D). Data are average of two experiments.

(F) Sensitive phenotype of 3×HA-Rfu1-overexpressing cells to AZC (azetidine-2-carboxylic acid). Cells were spotted on SC-Ura plates with the indicated concentrations of AZC and incubated at 25°C for 3 days.

(Figures 2B and S4). Therefore, disruption of *RFU1*, which causes increased production of monomeric Ub, appears to enhance substrate ubiquitination, resulting in marked accumulation of HMW ubiquitinated proteins when combined with a mutated component of the UPS, although yet unidentified events could also enhance ubiquitination in the double mutant.

Next, we examined whether overexpression of Rfu1 has the opposite effect of that observed in *Δrfu1* cells on the Ub profile. Indeed, overexpression of 3×HA-tagged Rfu1 in wild-type cells resulted in reduction of monomeric Ub and increase of free Ub chains (Figure 2C). In addition, overexpression of 3×HA-Rfu1 in *Δrfu1* cells restored free Ub chain formation.

The growth of yeast cells lacking the polyubiquitin gene (*UBI4*) is similar to that of wild-type cells over the normal range of growth temperatures (Finley et al., 1987). However, they are hypersensitive to certain stresses probably because *Δubi4* cells cannot maintain the required levels of Ub during stress. If Rfu1 inhibits the supply of monomeric Ubs, overexpression of Rfu1 should have similar effects to those observed in *Δubi4* cells. To test this, wild-type cells overexpressing 3×HA-Rfu1 or harboring an empty vector were spotted on a plate, incubated at 39.5°C for 17 hr, and then placed at 25°C. Cells overexpressing 3×HA-Rfu1 were more sensitive to the sustained heat treatment than control cells (Figures 2D and 2E). Moreover, cells overexpressing 3×HA-Rfu1 were more sensitive to azetidine-2-carboxylic acid (AZC), a toxic analog of proline, than control cells (Figure 2F). Based on these results, we speculated that Rfu1 regulates Ub homeostasis by inhibiting the production of monomeric Ub and by promoting the formation of free Ub chains.

During the course of these experiments, we noticed that 3×HA-Rfu1 overexpression also caused less accumulation of HMW ubiquitinated proteins in *cdc48-3* than vector expression (Figure 2C). Together with the findings of profound growth defect and high levels of HMW ubiquitinated proteins in the double mutants, an excess amount of ubiquitinated proteins may have toxic effects, and this may explain the isolation of *RFU1* in our screening. Consistent with this notion, overexpression of Ub caused growth retardation in *cdc48-3* and in *cdc48-3Δrfu1* cells (Figure S5).

Interaction of Rfu1 with Doa4

What is the molecular mechanism of Rfu1-mediated modulation of the levels of monomeric Ub and of free Ub chains? First, we tested the possibility that Rfu1 directly binds to free Ub chains. Recombinant proteins including MBP, MBP-Rfu1, MBP-Rpn10, and MBP-UQ1(UBA), a MBP fusion with the UBA domain of human ubiquilin 1, were prepared (Figure S6), and they were incubated with K48-linked or K63-linked Ub chains (Figure S7). An MBP pull-down assay showed MBP-Rpn10 binding to

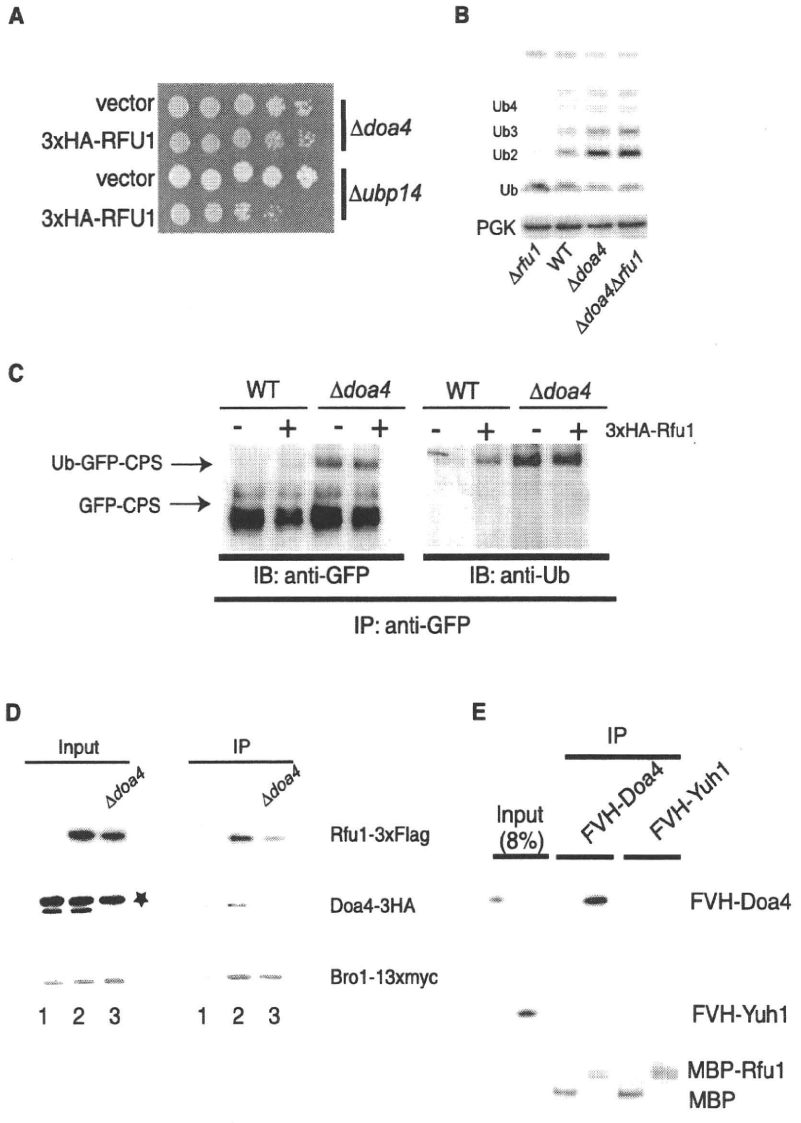

Figure 3. Rfu1 Interactions with Doa4

(A) Overexpression of 3×HA-Rfu1 inhibits the growth of *Δubp14* cells but not of *Δdoa4* cells.

(B) Resemblance of *Δdoa4Δrfu1* and *Δdoa4* mutants with regard to the level of monomeric Ub and Ub chains. *Top*, anti-Ub; *bottom*, anti-PGK immunoblot.

(C) Detection of ubiquitinated GFP-carboxypeptidase S (CPS) by overexpression of 3×HA-Rfu1 in control cells. Immunoprecipitation was performed using anti-GFP from control cells or *Δdoa4* cells expressing GFP-CPS with or without 3×HA-Rfu1. Immunocomplex was analyzed using anti-GFP and anti-Ub. Strains: Y703 and Y704 with plasmids pKU90 and E405 or vector.

(D) Association of Rfu1-3×Flag with Doa4-3×HA and Bro1-13×myc in vivo. Immunoprecipitation was performed using anti-Flag and the resulting immunocomplexes were analyzed by immunoblot using anti-Flag, anti-HA, and anti-myc. Lane 1: cells expressing nontagged Rfu1, Doa4-3×HA, and Bro1-13×myc (Y845); lane 2: cells expressing Rfu1-3×Flag, Doa4-3×HA, and Bro1-13×myc (Y860); lane 3: *Δdoa4* cells expressing Rfu1-3×Flag and Bro1-13×myc (Y862). Asterisk indicates nonspecific band for HA.

(E) In vitro binding between recombinant MBP or MBP-Rfu1 and FVH-Doa4 or FVH-Yuh1. MBP or MBP-Rfu1 was mixed with FVH-Doa4 or FVH-Yuh1, and the proteins were isolated with amylose resin. Samples were analyzed by immunoblot using anti-Flag and anti-MBP.

K48-linked Ub chains and MBP-UQ1(UBA) binding to K63-linked Ub chains as positive controls. However, MBP-Rfu1 bound to neither K48-linked nor K63-linked Ub chains (Figure S7).

In the next step, we speculated that Rfu1 could be related to DUBs based on the partial sequence similarity of Rfu1 and the two different DUBs. We then postulated that Rfu1 negatively regulates DUBs that catalyze the reaction of free Ub chains to monomeric Ub. A genome-wide analysis of GFP-fusion proteins of yeast has shown localization of Rfu1-GFP in the endosome (Huh et al., 2003). Among 19 DUBs in yeast including 16 UBP, 1 UCH, and 2 OTU, only Doa4, the yeast counterpart of human UBPY, is localized in the endosomes, in addition to the cytoplasm (Amerik et al., 2000b; Huh et al., 2003). Moreover, the *Δdoa4* mutant showed reduced levels of monomeric Ub and accumulation of small Ub species, (Dupre and Haguenauer-Tsapis, 2001; Nikko and Andre, 2007; Papa and Hochstrasser, 1993), which seems to be the opposite pattern of the Ub profile in *Δrfu1* cells. Interestingly, we found that the Ub profile of wild-type cells overexpressing an epitope-tagged Doa4 is similar to that of *Δrfu1* cells: high levels of monomeric Ub and massive reduction of free Ub chains (Figure S8). Based on these findings, we decided to test the possibility that Rfu1 is an inhibitor of Doa4.

We tried to obtain genetic evidence for the negative effect of Rfu1 on Doa4. Ubp14 is another DUB, which also plays a role in the control of free Ub chains, and the *Δubp14Δdoa4* double mutant was reported to show a synthetic growth defect (Amerik et al., 1997). We overexpressed 3×HA-Rfu1 in *Δubp14* and *Δdoa4* cells. If Rfu1 inhibits Doa4, Rfu1 overexpression would cause a growth defect in *Δubp14* cells, like that observed in *Δubp14Δdoa4*. Indeed, overexpression of 3×HA-Rfu1 caused a growth defect in *Δubp14* cells but not in *Δdoa4* cells (Figure 3A).

We also speculated that the altered Ub profile observed in *Δrfu1* mutant was due to elimination of Rfu1-mediated inhibition of Doa4. In this case, the Ub profile of *Δrfu1Δdoa4* cells should look like that of *Δdoa4* cells. Therefore, we compared the Ub profiles of *Δrfu1Δdoa4* and *Δdoa4* cells. As expected, in *Δrfu1Δdoa4* cells, the characteristic Ub pattern of *Δrfu1* was no longer observed; instead, its Ub pattern was quite similar to that of *Δdoa4* cells (Figure 3B). In contrast, the Ub profile of *Δrfu1Δubp14* showed a combined pattern of the two single mutants (Figure S9). These results indicate that Doa4 and Rfu1 control free Ub chains in the same pathway, whereas Ubp14 and Rfu1 regulate free Ub chains independently.

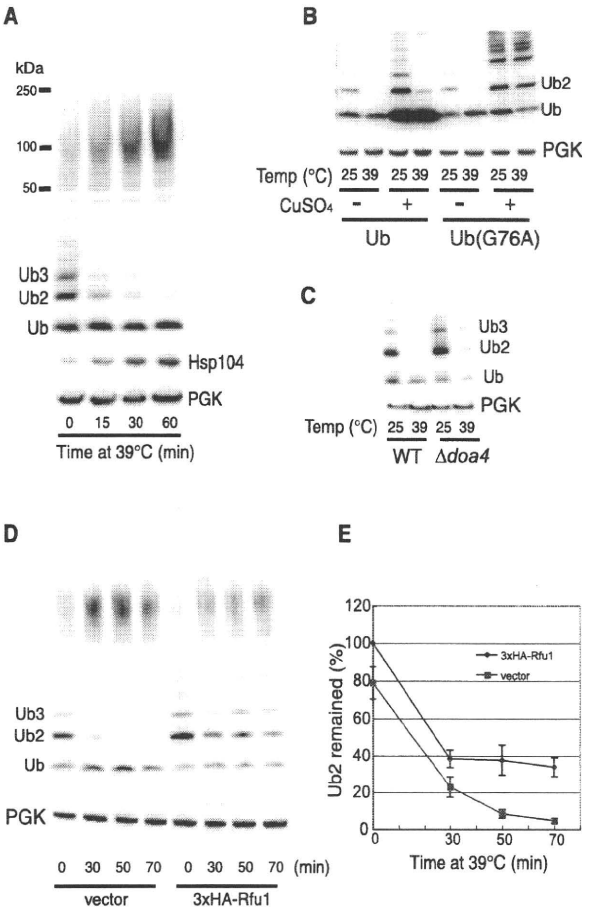

Figure 4. Free Ub Chains and Heat Shock Response

(A) Heat shock causes marked reduction in free Ub chains. Cells in early log phase at 25°C were heat shocked at 39°C at the indicated times. *Top*, anti-Ub; *middle*, anti-Hsp104; *bottom*, anti-PGK immunoblot.

(B) Resistance of Ub(G76A) chains to heat shock. Wild-type cells expressing CUP1-regulated monomeric Ub or Ub(G76A) were treated or not treated with 1 mM $CuSO_4$ for 4 hr and heat shocked at 39°C for 1 hr.

(C) Partial resistance of free Ub chains in *Δdoa4* cells to heat shock. Anti-Ub and anti-PGK immunoblot analyses were conducted for *Δdoa4* and wild-type cells. Cells were heat shocked at 39°C for 1 hr.

(D) Partial prevention of decrease of free Ub chains by overexpression of 3×HA-Rfu1. Cells harboring a vector or expressing 3×HA-Rfu1 were heat shocked at 39°C for 30, 50, and 70 min. *Top*, anti-Ub; *bottom*, anti-PGK.

(E) Relative Ub2 level observed in (D). Ub2 level in cells expressing 3×HA-Rfu1 is normalized to 100%. Data are mean ± SEM values of three independent experiments.

We then tested the involvement of Rfu1 in Doa4-mediated processes in vivo. Doa4 functions in a variety of cellular processes including the removal of polyubiquitin chain from Ub-conjugated proteins, which are targeted to proteasomes for degradation (Papa et al., 1999). Doa4 also controls DNA replication and protects cells against DNA damage (Fiorani et al., 2004; Singer et al., 1996). Moreover, *Δdoa4* mutant cells contain lower levels of monomeric Ub than the wild-type and exhibit accelerated degradation of monomeric Ub (Swaminathan et al., 1999). However, the major function of Doa4 is deubiquitination of ubiquitinated cargos sorted into luminal vesicles of late-endosomal multivesicular bodies (MVBs) (Amerik and Hochstrasser, 2004). In *Δdoa4* cells, cargo proteins such as carboxypeptidase S (CPS) accumulate in ubiquitinated forms (Dupre and Haguenauer-Tsapis, 2001; Katzmann et al., 2001). If Rfu1 inhibits the Doa4 activity, Rfu1 overexpression should result in phenocopying Δ*doa4* mutant on such proteins. Control and *Δdoa4* cells were transformed with two plasmids: a plasmid expressing GFP-CPS and another overexpressing 3×HA-Rfu1 or an empty vector. GFP-CPS was immunoprecipitated with anti-GFP antibody, and GFP-CPS and ubiquitinated GFP-CPS were detected by immunoblotting using anti-GFP and anti-Ub (Figure 3C). We used vacuolar proteases-deficient *Δpep4Δprb1* cells to facilitate the detection of the ubiquitinated form of GFP-CPS (Amerik et al., 2006). Consistent with previous results (Katzmann et al., 2001; Amerik et al., 2006), the ubiquitinated form of GFP-CPS was observed in *Δdoa4* cells. In addition, the ubiquitinated form of GFP-CPS was clearly observed in cells overexpressing 3×HA-Rfu1 but not in cells harboring the empty vector. These results added further support for the role of Rfu1 as an inhibitor of Doa4.

Next, we investigated whether Rfu1 physically interacts with Doa4 by immunoprecipitating the Rfu1-3×Flag protein from yeast cell lysates (Figure 3D). For this purpose, we created cells in which endogenous *RFU1* and *DOA4* were replaced with *RFU1-3×FLAG* and *DOA4-3×HA*, respectively. In addition, we replaced *BRO1* with *BRO1-13×MYC*. Bro1 is an endosome recruiting factor for Doa4: in the absence of Bro1, Doa4 localization to endosomes is abolished (Luhtala and Odorizzi, 2004). Bro1 also stimulates the Dub activity of Doa4 by direct binding (Richter et al., 2007). As shown in Figure 3D, Rfu1-3×Flag coimmunoprecipitated Doa4-3×HA as well as Bro1-13×myc (lane 2). However, Rfu1-3×Flag did not bind with Doa4-3×HA in Δ*bro1* cell (data not shown), perhaps due to a lower level of Rfu1-3×Flag in Δ*bro1* cells (data not shown), although other explanations are possible. Surprisingly, Bro1-13×myc was coimmunoprecipitated with Rfu1-3×Flag in the *Δdoa4* mutant, suggesting that Rfu1 binds Bro1 directly (Figure 3D, lane 3). These results indicate that Rfu1 forms a complex with Doa4 and Bro1.

We also investigated whether Rfu1 binds to Doa4 directly in vitro. N-terminal Flag-tagged and C-terminal V5- and His-tagged full-length Doa4 (FVH-Doa4) and Yuh1 (FVH-Yuh1) were expressed and purified from yeast (Figure S6). Yuh1 is another yeast DUB. FVH-Doa4 and FVH-Yuh1 were mixed with recombinant MBP or MBP-Rfu1 to investigate whether these tagged proteins bind to MBP or MBP-Rfu1. MBP-Rfu1, but not MBP, specifically bound to FVH-Doa4 but not FVH-Yuh1 (Figure 3E), indicating that Rfu1 physically interacts with Doa4.

Stress Response, Free Ub Chains, Doa4, and Rfu1

The Ub profile varies with the growth phase of yeasts. Free Ub chains are abundantly observed in log phase but not in stationary phase (Amerik et al., 1997 and data not shown). We speculated that the formation of free Ub chains depends on cellular conditions. To test this, we examined the effects of environmental stresses such as heat shock on the Ub profile. Wild-type cells were grown at 25°C to an early log phase and then heated at 39°C (Figure 4A). The heat treatment increased HMW ubiquitinated proteins, consistent with the previous findings in

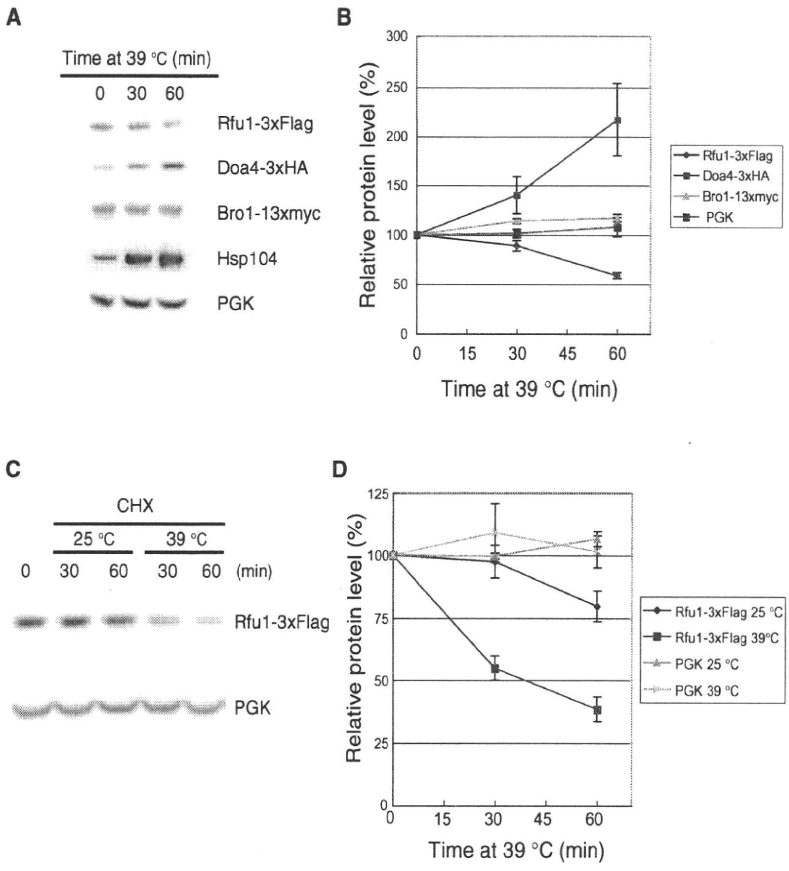

Figure 5. Rfu1-3×Flag, Doa4-3×HA, and Bro1-13×myc Protein Levels in Response to Heat Shock

(A) Rfu1-3×Flag, Doa4-3×HA, Bro1-13×myc, and PGK protein levels under heat shock at 39°C. Total cell lysates obtained at the indicated time points were analyzed by immunoblotting with anti-Flag, anti-HA, anti-myc, anti-Hsp104, and anti-PGK.

(B) Quantification of protein levels. Protein levels were quantified from the bands shown in (A). Data are mean ± SEM values of three independent experiments.

(C) Rfu1-3×flag and PGK protein levels under heat shock in the presence of cycloheximide.

(D) Quantification of protein levels. Protein levels were quantified from the bands shown in (C). Data are mean ± SEM values of three independent experiments.

mammalian cultured cells (Carlson et al., 1987). The heat treatment also resulted in marked increase in Hsp104 protein, one of the major heat-inducible proteins. Surprisingly, heat treatment resulted in disappearance of free Ub chains; their level decreased after 15 min of such treatment.

We speculated that one reason for the marked decrease in free Ub chains upon heat treatment was the disassembling of free Ub chains by certain DUBs to produce more monomeric Ub, which can be used for ubiquitination reactions. Accordingly, we examined the involvement of DUB activity in stress-induced disappearance of free Ub chains. Ub(G76A), in which the last amino acid of glycine in Ub is replaced with alanine, is reported to form a Ub chain, but it is resistant to the action of deubiquitinating enzymes (Hodgins et al., 1992). Plasmids expressing G76A monomeric Ub or wild-type monomeric Ub under the regulation of Cup1 promoter were introduced into wild-type cells (Figure 4B). In the absence of copper, when essentially only endogenous Ub-encoding genes were expressed, heat treatment markedly decreased the level of free Ub chains. Copper-induced exogenous wild-type Ub expression increased free Ub chains but decreased the chains upon heat shock. On the other hand, in cells expressing Ub(G76A), heat shock did not reduce the amount of small Ub oligomer-like species. Although we cannot exclude the possibility that the observed results are due to reasons other than that UbG76A is a poor substrate for DUBs, the above findings emphasize the potential involvement of DUB(s) in the disappearance of free Ub chains.

We further investigated whether Doa4 mediates the heat shock-induced decrease in free Ub chains. To test this, *Δdoa4* cells were heat shocked and the Ub profiles of the cells were examined. Compared with wild-type cells, substantial amounts of free Ub chains remained in *Δdoa4* cells even after 1 hr of heat shock (Figure 4C), suggesting the involvement of Doa4 in this process. Next, we examined the effect of 3×HA-Rfu1 overexpression. If Rfu1 inhibits Doa4, overexpression of 3×HA-Rfu1 should phenocopy *Δdoa4* mutant with respect to heat shock-induced disappearance of free Ub chains. Wild-type cells overexpressing 3×HA-Rfu1 were heat shocked, and the change in free Ub chains was examined. We found that overexpression of 3×HA-Rfu1 under the regulation of the glyceraldehyde-3-phosphate dehydrogenase (GPD) promoter significantly inhibited the disappearance of free Ub chains (Figures 4D and 4E). These results indicate that disappearance of free Ub chains is at least partly mediated by a balance of the actions of Doa4 and Rfu1.

Since the mRNA levels of *RFU1* and *DOA4* decrease and increase upon heat shock, respectively (Gasch et al., 2000), we decided to examine the effects of heat shock on the levels of their proteins. We found that the changes in Rfu1-3×Flag and Doa4-3×HA levels paralleled the reported changes in their mRNA levels upon heat treatment (Figures 5A and 5B). The amount of Rfu1-3×Flag decreased by 40%–50% after 60 min of heat shock. In contrast, heat shock increased the Doa4-3×HA level, though the increase was modest compared with the marked increase in the heat shock protein Hsp104. The level of Bro1-13×myc remained unchanged upon heat shock. These results were consistent with the notion that heat shock produces more Doa4 that is uninhibited by Rfu1and can thus contribute to disassembling free Ub chains.

We also tested whether decrease of Rfu1-3×Flag was also mediated at the protein level and thus examined the stability of Rfu-3×Flag. In cells treated with cycloheximide followed

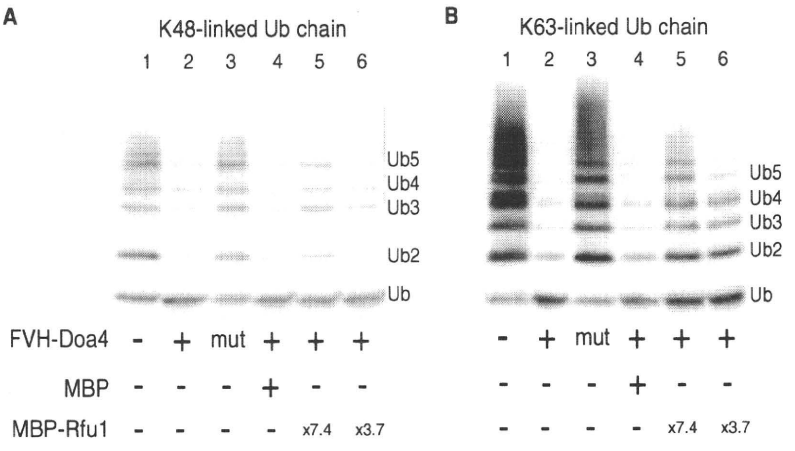

Figure 6. In Vitro Doa4 DUB Activity toward Ub Chains and Rfu1 Inhibition

(A and B) Detection of Doa4 DUB activity toward K48- or K63-linked Ub chains and inhibition by MBP-Rfu1. FVH-Doa4 (1.1 μg) and FVH-Doa4 (Cys571Ser) were added in lanes 2 and 3, respectively. MBP was added at 9.4-fold molar excess and MBP-Rfu1 was added at 7.4- and 3.7-fold molar excess to FVH-Doa4 (lanes 4, 5, and 6, respectively).

immediately by heat shock, Rfu1-3×Flag was rather stable at 25°C but became unstable upon heat shock (Figures 5C and 5D). This result indicated that the expression of Rfu1 is regulated both at mRNA and protein levels upon thermal stress.

Rfu1 Is an Inhibitor of Doa4 In Vitro

The above results suggested that Doa4 can disassemble free Ub chains to monomeric Ub, and that Rfu1 inhibits this activity. Next, we examined whether Doa4 can disassemble free Ub chains in vitro. We used K48-linked and K63-linked Ub chains as substrates because the linkage of Ub dimer purified from *Arabiodopsis* is Lys48-linked, and the linkage of free Ub chains purified from yeast expressing His-tagged Ub is mainly Lys48-linked, though also to some extent Lys63-linked (van Nocker and Vierstra, 1993; Xu and Peng, 2008). When FVH-Doa4 was incubated with K48-linked or K63-linked Ub chains, DUB activity was observed for K48-linked and, more effectively, for K63-linked Ub chains (Figures 6A and 6B, lane 2). These DUB activities were abolished with the catalytic mutant of Doa4 (Cys571Ser) (lane 3) (Papa and Hochstrasser, 1993). In the next experiment, we premixed MBP-Rfu1 or MBP with FVH-Doa4 and added K48- or K63-linked Ub chains to see whether MBP-Rfu1 has any inhibitory effect. The addition of MBP-Rfu1 markedly inhibited DUB activity for both K48- and K63-linked Ub chains in a dose-dependent manner (lanes 5 and 6). The inhibitory effect was not observed with MBP (lane 4). To test whether the inhibitory effect was specific to Doa4 (Figure S10), we purified a tagged Ubp14 (FVH-Ubp14) and its catalytic mutant FVH-Ubp14(Cys332Ser). FVH-Ubp14 showed very strong DUB activity toward Ub chains. The use of MBP-Rfu1 showed no inhibitory effect, indicating that the inhibitory effect of Rfu1 is specific to Doa4.

Since Rfu1 binds Bro1 in vivo (Figure 3D), it is possible that Rfu1-Bro1 complexes may be a contaminant in these experiments that inhibit FVH-Doa4. To exclude this possibility, we purified FVH-Doa4 from *Δbro1Δdoa4Δpep4* cells and retested in vitro assays with the FVH-Doa4. The FVH-Doa4 from *Δbro1Δdoa4Δpep4* cells bound to MBP-Rfu1 and inhibited Doa4 DUB activity (Figure S11). These results indicate that Rfu1 directly inhibits the DUB activity of Doa4 in vitro.

DISCUSSION

Ub is used in numerous critical cellular events whereas monomeric Ub must be maintained at an adequate level at all times in response to different cellular conditions. Cells are equipped with defined systems to regulate monomeric Ub level (Finley et al., 1987; Hanna et al., 2007). Our analyses and results revealed a mechanism that regulates and maintains Ub levels; the balance of activities of DUB and its regulators determines the level of monomeric Ub. We propose that unanchored Ub chains function as a reservoir for monomeric Ub, as illustrated in Figure 7.

Rfu1 as an Inhibitor of Doa4

Based on the genetic and biochemical evidence provided in this study, we conclude that Rfu1 functions as an inhibitor of Doa4. Although several activators/inhibitors of DUBs have been reported (Ventii and Wilkinson, 2008), Rfu1 appears to provide the first example of inhibition of DUB both in vivo and in vitro. Since Doa4 functions in various important events, it is likely important to regulate Doa4 activity appropriately. Indeed, since Bro1 is an activator of Doa4 (Luhtala and Odorizzi, 2004; Richter et al., 2007), Doa4 is regulated by both an activator and an inhibitor. The exact molecular mechanism of Rfu1-induced Doa4 inhibition remains to be clarified, and this will elucidate how Rfu1 and Bro1 coordinate to regulate Doa4 activity. Bro1 recruits Doa4 through the interaction of the N-terminal noncatalytic region of Doa4, and Bro1 stimulates the deubiquitination activity of Doa4 through the interaction of the C-terminal catalytic region (Richter et al., 2007). For Doa4 to exhibit its function, it is important that it localizes in the endosome, a process dependent on Bro1 (Amerik et al., 2006; Richter et al., 2007). Based on the finding that Bro1 binds to Rfu1 in the absence of Doa4, we speculate that Bro1 also recruits Rfu1 to the endosome. Indeed, the localization of Rfu1-GFP in the endosome was largely lost in the *Δbro1* mutant (Y.K. and K.T., unpublished data). Preliminary experiments provided evidence against any role for Rfu1 in recruiting Doa4 to the endosomes; Doa4-GFP localization remained unchanged following the introduction of *Δrfu1* mutation in the *Δvps4* mutant (Y.K. and K.T., unpublished data). These results, together with the present observation of direct inhibition of Doa4 by Rfu1 in vitro (Figure 6), indicate that Rfu1 could act on Doa4 to inhibit its activity after Bro1 recruits Doa4 to the endosome. Indeed, Bro1 is about 25-fold more abundant than Doa4 and Rfu1 (Ghaemmaghami et al., 2003) and hence potentially has many roles in the cell. It should be noted that we cannot

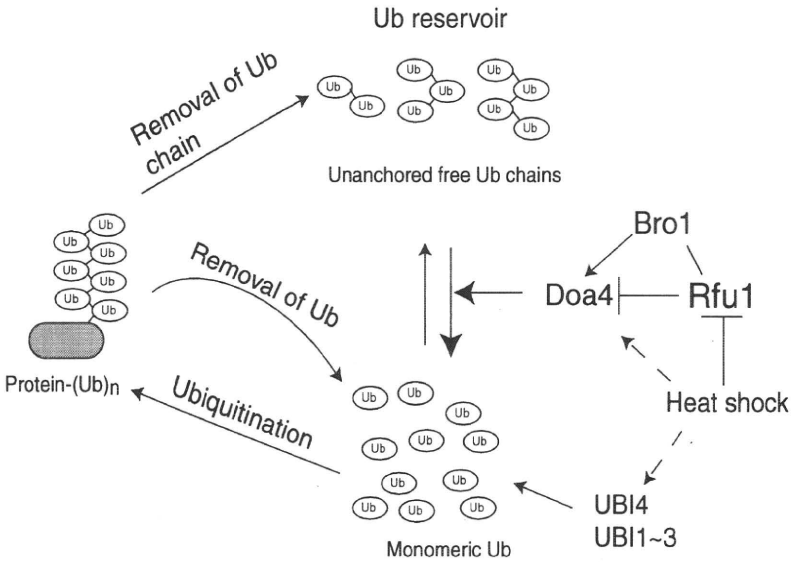

Figure 7. A Model of Regulation of Ub Homeostasis by Free Ub Chains

The monomeric ubiquitin (Ub) pool is maintained through synthesis from Ub-encoding genes, *UBI1–4*, by release from protein-conjugated Ub chains, and by release from free Ub chains. DUB(s), such as Doa4, supply monomeric Ub by cleaving free Ub chains. Under normal conditions, Rfu1 inhibits the activity of Doa4, resulting in the maintenance of the monomeric Ub pool, and consequently enhances the formation of free Ub chains. Upon heat shock, Rfu1 levels decrease and more Doa4 is produced (Figures 5A and 5B); therefore, monomeric Ub would be produced from free Ub chains by Doa4. In addition, transcription of *UBI4*-encoding polyubiquitin is increased. Since the activity of Doa4 is enhanced by Bro1, Doa4 would be controlled by a balance between its activator (e.g., Bro1) and inhibitor (e.g., Rfu1). Note that Bro1 is physically associated with Rfu1 (for details, see text).

exclude other functions for Rfu1 such as inhibition of Bro1 activity.

Rfu1 does not have any orthologs in higher eukaryotes. However, it has low sequence similarity to two different mammalian DUBs: AMSH and UBPY. The homologous regions lie mainly outside of the catalytic domains. Given that the homologous sequence is involved in the inhibition activity, the corresponding regions of AMSH and UBPY may also inhibit other DUBs or their own DUB activity.

Free Ub Chains, Doa4, Rfu1, and Heat Shock

More Ubs are required upon stress, probably due to the massive need of ubiquitination to degrade denatured proteins by the 26S proteasome (Finley et al., 1987). We showed that heat shock markedly decreased the levels of free Ub chains. We believe that production of monomeric Ub is regulated through deubiquitination activities and that heat stress increases monomeric Ub production by disassembling free Ub chains. Doa4 and Rfu1 are involved, even only in part, in this regulation, based on the following observations. First, Ub chains derived from Ub(G76A) remained after heat shock, suggesting the involvement of deubiquitination in the decrease of free Ub chains (Figure 4B). Second, overproduction of Doa4 into wild-type cells increased monomeric Ubs and decreased unanchored Ub chains (Figure S8), suggesting that Doa4 disassembles free Ub chains in vivo. Third, Doa4 indeed disassembled free Ub chains in vitro (Figure 6). Fourth, in Δ*doa4* mutant and wild-type cells overexpressing 3×HA-Rfu1, free Ub chains partly remained upon heat shock (Figures 4C–4E). Fifth, heat shock decreased Rfu1 and increased Doa4 protein levels (Figure 5A). However, in addition to Doa4, another DUB(s) may contribute to the disappearance of free Ub chains upon heat shock since the effects of Δ*doa4* mutation and Rfu1 overexpression were far from complete. DUBs whose mutants show altered Ub profile may be good candidates. The next challenge is to identify other heat-stress-responsive proteins that contribute to the decrease in free Ub chains.

It could be argued that the disappearance of Ub chains upon heat shock is caused by the direct use of Ub chains to a substrate. Recent studies have shown that E2-charged polyubiquitin chains can be directly transferred to a substrate (Li et al., 2007; Ravid and Hochstrasser, 2007). However, this mechanism does not appear to be applied at heat shock because we confirmed that free Ub chains are not E2 charged: yeast lysate treated with dithiothreitol (DTT), a reducing reagent, and DTT-untreated lysate, which should retain the thioester-linkage with E2, showed a similar Ub profile (data not shown).

Increase of Doa4-3×HA and decrease of Rfu1-3×Flag proteins were observed upon heat shock. Heat shock also changes the mRNA levels of *DOA4* and *RFU1* (Gasch et al., 2000). Several genes involved in ribosome transport and assembly show mRNA expression patterns similar to that of *RFU1* upon heat stress (Gasch et al., 2000). Synthesis of many ribosomal proteins is sensitive to high temperature, thus explaining the drop in protein synthesis upon heat shock (Woolford and Warner, 1991). The regulation of Rfu1 expression may be under a similar control. In addition to the regulation of mRNA, we found that heat shock specifically degraded Rfu1-3×Flag protein. Thus, the expression of Rfu1 is regulated by both mRNA and protein levels. We are currently investigating the system involved in Rfu1 protein degradation.

Unanchored Ub Chains as a Reservoir for Monomeric Ub?

If we apply the scenario of disassembling of free Ub chains by DUBs, one can assume that free Ub chains function not only as inhibitors of the 26S proteasome as proposed previously (Amerik et al., 1997) but also as a reservoir for Ubs, which can rapidly provide the cell with monomeric Ubs when more Ub is needed, such as under various stress conditions or stimuli (e.g., heat, chemical treatments, electronic pulses, etc.) (Figure 7). Alternatively, keeping Ubs in the form of free Ub chains may be an efficient way to reduce excess monomeric Ubs, thus preventing unnecessary ubiquitination of cellular proteins.

Consistent with this hypothesis, the double mutants of *Δrfu1* and a component of the UPS (*cdc48-3, ΔN rpn2, rpt1/cim5-1*) contained much more HMW ubiquitinated proteins and were more sensitive to higher temperatures than the single mutant (Figures 1C–1E, 2B, and S4). As more monomeric Ubs are provided by disruption of *RFU1*, overload of the ubiquitination process would occur in the *Δrfu1* mutant and may result in further accumulation of HMW ubiquitinated proteins in the double mutants. Consistently, Ub overproduction was toxic to *cdc48-3* and *cdc48-3Δrfu1* cells (Figure S5). Conversely, overexpression of *RFU1* suppressed the temperature-sensitive growth phenotype of *cdc48-3*, in which Rfu1 was originally isolated in the screening, as well as decreased accumulation of HMW ubiquitinated proteins in *cdc48-3* (Figures 1B and 2C). Thus, consistent with a previous report (London et al., 2004), these ubiquitinated proteins probably cause damage to cells, leading to sensitivity to elevated temperatures. The concept of a free Ub chain acting as a Ub reservoir is reminiscent of glycogen as a storage form of glucose (Stryer, 1981). Excess glucose is stored in the form of glycogen, a chained form of glucose, to maintain glucose concentration in blood at adequate levels. When more glucose is required, glycogen is rapidly hydrolyzed to produce glucose.

As a candidate checkpoint factor for Ub homeostasis, further exploration of the molecular function of Rfu1 will certainly provide a better understanding of Ub homeostasis and of the stress response. Moreover, since free Ub chains exist in various organisms (van Nocker and Vierstra, 1993), it is conceivable that regulation of Ub homeostasis by free Ub chains is a universal mechanism.

EXPERIMENTAL PROCEDURES

Immunoblotting

Preparation of whole-cell extracts and immunoblot analysis were performed essentially as described previously (Kimura et al., 2001), except cells were harvested in the early log phase. To determine the effect of 3×HA-Rfu1 overexpression on Ub profile and stress tolerance, fresh colonies after plasmid transformation were directly suspended in medium and cultured. To analyze the overall Ub profile, total cell proteins were separated by 4%–20% or 10%–20% gradient gels (Bio-Rad, Hercules, CA, USA) using glycine- or tricine-based buffer, followed by transfer to Immobilon-P membranes (Millipore, Bedford, MA, USA). Blots were incubated with mouse anti-Ub monoclonal antibody, MAB1510 (Chemicon International, Inc., Temecula, CA, USA), anti-HA antibody (HA.11, COVANCE, Princeton, NJ, USA), or anti-yeast PGK antibody (Molecular Probes, Eugene, OR, USA), followed by horseradish peroxidase (HRP)-conjugated anti-mouse IgG (#NA931V Amersham Biosciences, Arlington Heights, IL, USA), and detected using ECL-plus reagents (Amersham Biosciences). Rabbit anti-Hsp104 antibody was purchased from Stressgen (Ann Arbor, MI, USA).

Immunoprecipitation

For immunoprecipitation of Rfu1-3×Flag, cells were grown to early logarithmic phase and harvested by centrifugation. Cells were lysed in buffer A (10 mM Tris HCl, pH 7.5, 50 mM potassium acetate, 2 mM EDTA, 10% glycerol, 5 μg/ml pepstatin A, and protease inhibitor cocktail [Roche]) with multi-beads shocker (Yasui Kikai), and Triton X-100 was added at a final concentration of 0.5%. Lysates were centrifuged and the supernatant was incubated with anti-Flag M2 agarose (Sigma) for 2 hr in cold room. After washing with buffer A plus 0.5% Triton X-100, the immunocomplex was eluted by 1× sample buffer and analyzed by western blotting. The blots were incubated with anti-HA, anti-myc (9E10, Santa Cruz Biotechnology), or anti-Flag antibody (Sigma).

For immunoprecipitation of GFP-CPS, cells were lysed in buffer A with a multi-beads shocker. After centrifugation, the supernatants were incubated with anti-GFP antibody (Roche) and Protein G sepharose. The immunocomplex was washed with buffer A plus 1% Triton X-100 and 200 mM NaCl, eluted with 1× sample buffer, and analyzed by western blotting.

In Vitro Binding of MBP-Rfu1 with FVH-Doa4

Maltose-binding protein (MBP) or MBP-Rfu1 (each 5 μg) was mixed with FVH-Doa4 or FVH-Yuh1 (each 4 μg) in buffer B (50 mM Tris-HCl, pH 7.5, 100 mM NaCl, 10% glycerol, and 0.5% Triton X-100) for 1 hr at 25°C followed by the addition of amylose resin. After 30 min, the resin was washed with buffer B and eluted with buffer B containing 10 mM maltose. The eluted samples were analyzed by western blotting.

In Vitro Doa4 Deubiquitinating Assay

The DUB activity of FVH-Doa4 and its mutant was tested with K48-linked and K63-linked polyubiquitin (Biomol International, 1 μg each per reaction) in 100 mM Tris-HCl, pH 7.5, 100 mM KCl, 100 mM $MgCl_2$, 100 mM DTT, and 1.9% glycerol. To determine the effect of MBP-Rfu1 or MBP, the proteins were mixed with FVH-Doa4 for 15 min prior to the addition of polyubiquitin. Reactions were incubated for 2 or 3 hr at 25°C, mixed with a sample buffer, and heated at 37°C for 30 min. They were analyzed by immunoblotting using anti-Ub antibody (P4D1).

SUPPLEMENTAL DATA

Supplemental Data include Supplemental Experimental Procedures, 11 figures, 2 tables, and Supplemental References and can be found with this article online at http://www.cell.com/supplemental/S0092-8674(09)00204-9.

ACKNOWLEDGMENTS

We thank T. Fujita for his initial support and C. Takahashi, H. Ueno, and T. Hasegawa for technical support. We also thank D. Botstein, K. Matsumoto, K. Umebayashi, R. Hirata, A. Nakano, Y. Saeki, S. Ito, and A. Amerik for materials, Y. Saeki, K. Umebayashi, R. Hirata, A. Nakano, A. Toh-e, Y. Yoshida, and N. Matsuda for discussion, and A. Toh-e for comments on the manuscript. This work was supported by Grants-in-Aid for Scientific Research on Priority Area (to Y.K.), Specially Promoted Research (to K.T.) from the Ministry of Education, Culture, Science and Technology of Japan, the Target Protein Project of MEXT (to K.T.), and Takeda Science Foundation (to K.T.).

Received: November 30, 2007
Revised: November 14, 2008
Accepted: February 6, 2009
Published: April 30, 2009

REFERENCES

Amerik, A.Y., and Hochstrasser, M. (2004). Mechanism and function of deubiquitinating enzymes. Biochim. Biophys. Acta *1695*, 189–207.

Amerik, A., Swaminathan, S., Krantz, B.A., Wilkinson, K.D., and Hochstrasser, M. (1997). In vivo disassembly of free polyubiquitin chains by yeast Ubp14 modulates rates of protein degradation by the proteasome. EMBO J. *16*, 4826–4838.

Amerik, A.Y., Li, S.J., and Hochstrasser, M. (2000a). Analysis of the deubiquitinating enzymes of the yeast *Saccharomyces cerevisiae*. Biol. Chem. *381*, 981–992.

Amerik, A.Y., Nowak, J., Swaminathan, S., and Hochstrasser, M. (2000b). The Doa4 deubiquitinating enzyme is functionally linked to the vacuolar protein-sorting and endocytic pathways. Mol. Biol. Cell *11*, 3365–3380.

Amerik, A., Sindhi, N., and Hochstrasser, M. (2006). A conserved late endosome-targeting signal required for Doa4 deubiquitylating enzyme function. J. Cell Biol. *175*, 825–835.

Carlson, N., Rogers, S., and Rechsteiner, M. (1987). Microinjection of ubiquitin: changes in protein degradation in HeLa cells subjected to heat-shock. J. Cell Biol. *104*, 547–555.

Chen, Y., and Piper, P.W. (1995). Consequences of the overexpression of ubiquitin in yeast: elevated tolerances of osmostress, ethanol and canavanine, yet reduced tolerances of cadmium, arsenite and paromomycin. Biochim. Biophys. Acta *1268*, 59–64.

Chernova, T.A., Allen, K.D., Wesoloski, L.M., Shanks, J.R., Chernoff, Y.O., and Wilkinson, K.D. (2003). Pleiotropic effects of Ubp6 loss on drug sensitivities and yeast prion are due to depletion of the free ubiquitin pool. J. Biol. Chem. *278*, 52102–52115.

Dupre, S., and Haguenauer-Tsapis, R. (2001). Deubiquitination step in the endocytic pathway of yeast plasma membrane proteins: crucial role of Doa4p ubiquitin isopeptidase. Mol. Cell. Biol. *21*, 4482–4494.

Finley, D., Ozkaynak, E., and Varshavsky, A. (1987). The yeast polyubiquitin gene is essential for resistance to high temperatures, starvation, and other stresses. Cell *48*, 1035–1046.

Fiorani, P., Reid, R.J., Schepis, A., Jacquiau, H.R., Guo, H., Thimmaiah, P., Benedetti, P., and Bjornsti, M.A. (2004). The deubiquitinating enzyme Doa4p protects cells from DNA topoisomerase I poisons. J. Biol. Chem. *279*, 21271–21281.

Gasch, A.P., Spellman, P.T., Kao, C.M., Carmel-Harel, O., Eisen, M.B., Storz, G., Botstein, D., and Brown, P.O. (2000). Genomic expression programs in the response of yeast cells to environmental changes. Mol. Biol. Cell *11*, 4241–4257.

Ghaemmaghami, S., Huh, W.K., Bower, K., Howson, R.W., Belle, A., Dephoure, N., O'Shea, E.K., and Weissman, J.S. (2003). Global analysis of protein expression in yeast. Nature *425*, 737–741.

Ghislain, M., Udvardy, A., and Mann, C. (1993). S. cerevisiae 26S protease mutants arrest cell division in G2/metaphase. Nature *366*, 358–362.

Ghislain, M., Dohmen, R.J., Levy, F., and Varshavsky, A. (1996). Cdc48p interacts with Ufd3p, a WD repeat protein required for ubiquitin-mediated proteolysis in Saccharomyces cerevisiae. EMBO J. *15*, 4884–4899.

Hanna, J., Meides, A., Zhang, D.P., and Finley, D. (2007). A ubiquitin stress response induces altered proteasome composition. Cell *129*, 747–759.

Hershko, A., and Ciechanover, A. (1998). The ubiquitin system. Annu. Rev. Biochem. *67*, 425–479.

Hodgins, R.R., Ellison, K.S., and Ellison, M.J. (1992). Expression of a ubiquitin derivative that conjugates to protein irreversibly produces phenotypes consistent with a ubiquitin deficiency. J. Biol. Chem. *267*, 8807–8812.

Huh, W.K., Falvo, J.V., Gerke, L.C., Carroll, A.S., Howson, R.W., Weissman, J.S., and O'Shea, E.K. (2003). Global analysis of protein localization in budding yeast. Nature *425*, 686–691.

Isono, E., Nishihara, K., Saeki, Y., Yashiroda, H., Kamata, N., Ge, L., Ueda, T., Kikuchi, Y., Tanaka, K., Nakano, A., and Toh-e, A. (2007). The assembly pathway of the 19S regulatory particle of the yeast 26S proteasome. Mol. Biol. Cell *18*, 569–580.

Johnson, E.S., Ma, P.C.M., Ota, I.M., and Varshavsky, A. (1995). A proteolytic pathway that recognizes ubiquitin as a degradation signal. J. Biol. Chem. *270*, 17422–17456.

Katzmann, D.J., Babst, M., and Emr, S.D. (2001). Ubiquitin-dependent sorting into the multivesicular body pathway requires the function of a conserved endosomal protein sorting complex, ESCRT-I. Cell *106*, 145–155.

Kimura, Y., Koitabashi, S., Kakizuka, A., and Fujita, T. (2001). Initial process of polyglutamine aggregate formation in vivo. Genes Cells *6*, 887–897.

Li, W., Tu, D., Brunger, A.T., and Ye, Y. (2007). A ubiquitin ligase transfers preformed polyubiquitin chains from a conjugating enzyme to a substrate. Nature *446*, 333–337.

London, M.K., Keck, B.I., Ramos, P.C., and Dohmen, R.J. (2004). Regulatory mechanisms controlling biogenesis of ubiquitin and proteasome. FEBS Lett. *567*, 259–264.

Luhtala, N., and Odorizzi, G. (2004). Bro1 coordinates deubiquitination in the multivesicular body pathway by recruiting Doa4 to endosomes. J. Cell Biol. *166*, 717–729.

McCullough, J., Clague, M.J., and Urbe, S. (2004). AMSH is an endosome-associated ubiquitin isopeptidase. J. Cell Biol. *166*, 487–492.

Mukhopadhyay, D., and Riezman, H. (2007). Proteasome-independent functions of ubiquitin in endocytosis and signaling. Science *315*, 201–205.

Naviglio, S., Mattecucci, C., Matoskova, B., Nagase, T., Nomura, N., Di Fiore, P.P., and Draetta, G.F. (1998). UBPY: a growth-regulated human ubiquitin isopeptidase. EMBO J. *17*, 3241–3250.

Nikko, E., and Andre, B. (2007). Evidence for a direct role of the Doa4 deubiquitinating enzyme in protein sorting into the MVB pathway. Traffic *8*, 566–581.

Osaka, H., Wang, Y.L., Takada, K., Takizawa, S., Setsuie, R., Li, H., Sato, Y., Nishikawa, K., Sun, Y.J., Sakurai, M., et al. (2003). Ubiquitin carboxy-terminal hydrolase L1 binds to and stabilizes monoubiquitin in neuron. Hum. Mol. Genet. *12*, 1945–1958.

Papa, F.R., and Hochstrasser, M. (1993). The yeast DOA4 gene encodes a deubiquitinating enzyme related to a product of the human tre-2 oncogene. Nature *366*, 313–319.

Papa, F.R., Amerik, A.Y., and Hochstrasser, M. (1999). Interaction of the Doa4 deubiquitinating enzyme with the yeast 26S proteasome. Mol. Biol. Cell *10*, 741–756.

Pickart, C.M., and Eddins, M.J. (2004). Ubiquitin: structures, functions, mechanisms. Biochim. Biophys. Acta *1695*, 55–72.

Ravid, T., and Hochstrasser, M. (2007). Autoregulation of an E2 enzyme by ubiquitin-chain assembly on its catalytic residue. Nat. Cell Biol. *9*, 422–427.

Richter, C., West, M., and Odorizzi, G. (2007). Dual mechanisms specify Doa4-mediated deubiquitination at multivesicular bodies. EMBO J. *26*, 2454–2464.

Row, P.E., Liu, H., Hayes, S., Welchman, R., Charalabous, P., Hofmann, K., Clague, M.J., Sanderson, C.M., and Urbe, S. (2007). The MIT domain of UBPY constitutes a CHMP binding and endosomal localization signal required for efficient epidermal growth factor receptor degradation. J. Biol. Chem. *282*, 30929–30937.

Ryu, K.Y., Maehr, R., Gilchrist, C.A., Long, M.A., Bouley, D.M., Mueller, B., Ploegh, H.L., and Kopito, R.R. (2007). The mouse polyubiquitin gene UbC is essential for fetal liver development, cell-cycle progression and stress tolerance. EMBO J. *26*, 2693–2706.

Ryu, K.Y., Garza, J.C., Lu, X.Y., Barsh, G.S., and Kopito, R.R. (2008). Hypothalamic neurodegeneration and adult-onset obesity in mice lacking the Ubb polyubiquitin gene. Proc. Natl. Acad. Sci. USA *105*, 4016–4021.

Schnell, J.D., and Hicke, L. (2003). Non-traditional functions of ubiquitin and ubiquitin-binding proteins. J. Biol. Chem. *278*, 35857–35860.

Singer, J.D., Manning, B.M., and Formosa, T. (1996). Coordinating DNA replication to produce one copy of the genome requires genes that act in ubiquitin metabolism. Mol. Cell. Biol. *16*, 1356–1366.

Stryer, L. (1981). Biochemistry, Second Edition (New York: W.H. Freeman and Company).

Swaminathan, S., Amerik, A.Y., and Hochstrasser, M. (1999). The Doa4 deubiquitinating enzyme is required for ubiquitin homeostasis in yeast. Mol. Biol. Cell *10*, 2583–2594.

van Nocker, S., and Vierstra, R.D. (1993). Multiubiquitin chains linked through lysine 48 are abundant in vivo and are competent intermediates in the ubiquitin proteolytic pathway. J. Biol. Chem. *268*, 24766–24773.

Ventii, K.H., and Wilkinson, K.D. (2008). Protein partners of deubiquitinating enzymes. Biochem. J. *414*, 161–175.

Woodman, P.G. (2003). p97, a protein coping with multiple identities. J. Cell Sci. *116*, 4283–4290.

Woolford, J.J., and Warner, J.R. (1991). The ribosome and its synthesis. In The Molecular and Cellular Biology of the Yeast Saccharomyces, J.R. Broach, J.R. Pringle, and E.W. Jones, eds. (Cold Spring Harbor, NY: Cold Spring Harbor Laboratory Press), pp. 587–626.

Xu, P., and Peng, J. (2008). Characterization of polyubiquitin chain structure by middle-down mass spectrometry. Anal. Chem. *80*, 3438–3444.

nature cell biology

The selective autophagy substrate p62 activates the stress responsive transcription factor Nrf2 through inactivation of Keap1

Masaaki Komatsu[1,2,8], Hirofumi Kurokawa[3], Satoshi Waguri[4], Keiko Taguchi[3], Akira Kobayashi[5], Yoshinobu Ichimura[1,6], Yu-Shin Sou[1,6], Izumi Ueno[1], Ayako Sakamoto[1], Kit I. Tong[3], Mihee Kim[5], Yasumasa Nishito[1], Shun-ichiro Iemura[7], Tohru Natsume[7], Takashi Ueno[6], Eiki Kominami[6], Hozumi Motohashi[3], Keiji Tanaka[1,8] and Masayuki Yamamoto[3,8]

Impaired selective turnover of p62 by autophagy causes severe liver injury accompanied by the formation of p62-positive inclusions and upregulation of detoxifying enzymes. These phenotypes correspond closely to the pathological conditions seen in human liver diseases, including alcoholic hepatitis and hepatocellular carcinoma. However, the molecular mechanisms and pathophysiological processes in these events are still unknown. Here we report the identification of a novel regulatory mechanism by p62 of the transcription factor Nrf2, whose target genes include antioxidant proteins and detoxification enzymes. p62 interacts with the Nrf2-binding site on Keap1, a component of Cullin-3-type ubiquitin ligase for Nrf2. Thus, an overproduction of p62 or a deficiency in autophagy competes with the interaction between Nrf2 and Keap1, resulting in stabilization of Nrf2 and transcriptional activation of Nrf2 target genes. Our findings indicate that the pathological process associated with p62 accumulation results in hyperactivation of Nrf2 and delineates unexpected roles of selective autophagy in controlling the transcription of cellular defence enzyme genes.

Macroautophagy (hereafter referred to as autophagy) is a highly conserved bulk protein degradation pathway responsible for the turnover of long-lived proteins, the disposal of excess or damaged organelles, and the clearance of aggregation-prone proteins. Isolation membranes engulf the cytoplasmic constituents, and the resulting autophagosomes fuse with lysosomes, resulting in complete degradation of the sequestered cytoplasmic components by lysosomal hydrolases[1]. Thus, inactivation of autophagy leads to cytoplasmic protein inclusions, which are composed of degenerated proteins, and the excess accumulation of deformed organelles, leading to liver injury[2], diabetes[3,4], heart disease[5] and neurodegeneration[6,7].

Although autophagy has generally been considered non-selective, growing lines of evidence indicate the selectivity of autophagy in sorting vacuolar enzymes such as aminopeptidase I and α-mannosidase[8] and in the removal of aggregation-prone proteins[9], unwanted organelles[10,11], and microbes[12]. Such selectivity by autophagy enables various methods of cellular regulation, as is well known for the ubiquitin proteasome pathway. The protein p62, which binds ubiquitin and LC3 (refs 13–15) and is a selective substrate for autophagy, regulates the formation of protein aggregates. Genetic ablation of *p62* suppressed the appearance of ubiquitin-positive protein aggregates in autophagy-deficient mice[16] and flies[17], indicating that p62 is important in the formation of inclusion bodies. Moreover, loss of *p62* markedly attenuated liver injury accompanied by the robust induction of antioxidant proteins resulting from autophagy deficiency[16]. This implies that impaired turnover of p62 is a major cause of the pathogenic changes seen in the livers of autophagy-deficient mice. Importantly, excess accumulation of p62 and inclusion bodies containing both ubiquitylated proteins and p62 have been identified in several human disorders, especially in neurodegenerative diseases[18], liver injuries[19] and hepatocellular carcinoma[20]. However, the molecular functions of p62 in autophagy-deficient conditions and its pathophysiological roles in human disorders are still unknown.

The Nrf2–Keap1 system is currently recognized as one of the main cellular defence mechanisms against oxidative and electrophilic stresses[21–23]. Under quiescent conditions, the transcription factor Nrf2 (nuclear factor erythroid 2-related factor 2) is constitutively degraded through the ubiquitin–proteasome pathway because its binding partner Keap1

[1]Laboratory of Frontier Science, Tokyo Metropolitan Institute of Medical Science, Bunkyo-ku, Tokyo 113-8613, Japan. [2]PRESTO, Japan Science and Technology Corporation, Kawaguchi 332-0012, Japan. [3]Department of Medical Biochemistry and ERATO-JST, Tohoku University Graduate School of Medicine, Aoba-ku, Sendai 980-8575, Japan. [4]Department of Anatomy and Histology, Fukushima Medical University School of Medicine, Hikarigaoka, Fukushima 960-1295, Japan. [5]Department of Medical Life Systems, Doshisha University, Kyoutanabe, Kyoto 610-0394, Japan. [6]Department of Biochemistry, Juntendo University School of Medicine, Bunkyo-ku, Tokyo 113-8421, Japan. [7]National Institutes of Advanced Industrial Science and Technology, Biological Information Research Center (JBIRC), Kohtoh-ku, Tokyo 135-0064, Japan.
[8]Correspondence should be addressed to M.K., K.T. or M.Y. (e-mail: komatsu-ms@igakuken.or.jp; tanaka-kj@igakuken.or.jp; masiyamamoto@m.tains.tohoku.ac.jp).

Received 19 November 2009; accepted 1 February 2010; published online 21 February 2010; DOI:10.1038/ncb2021

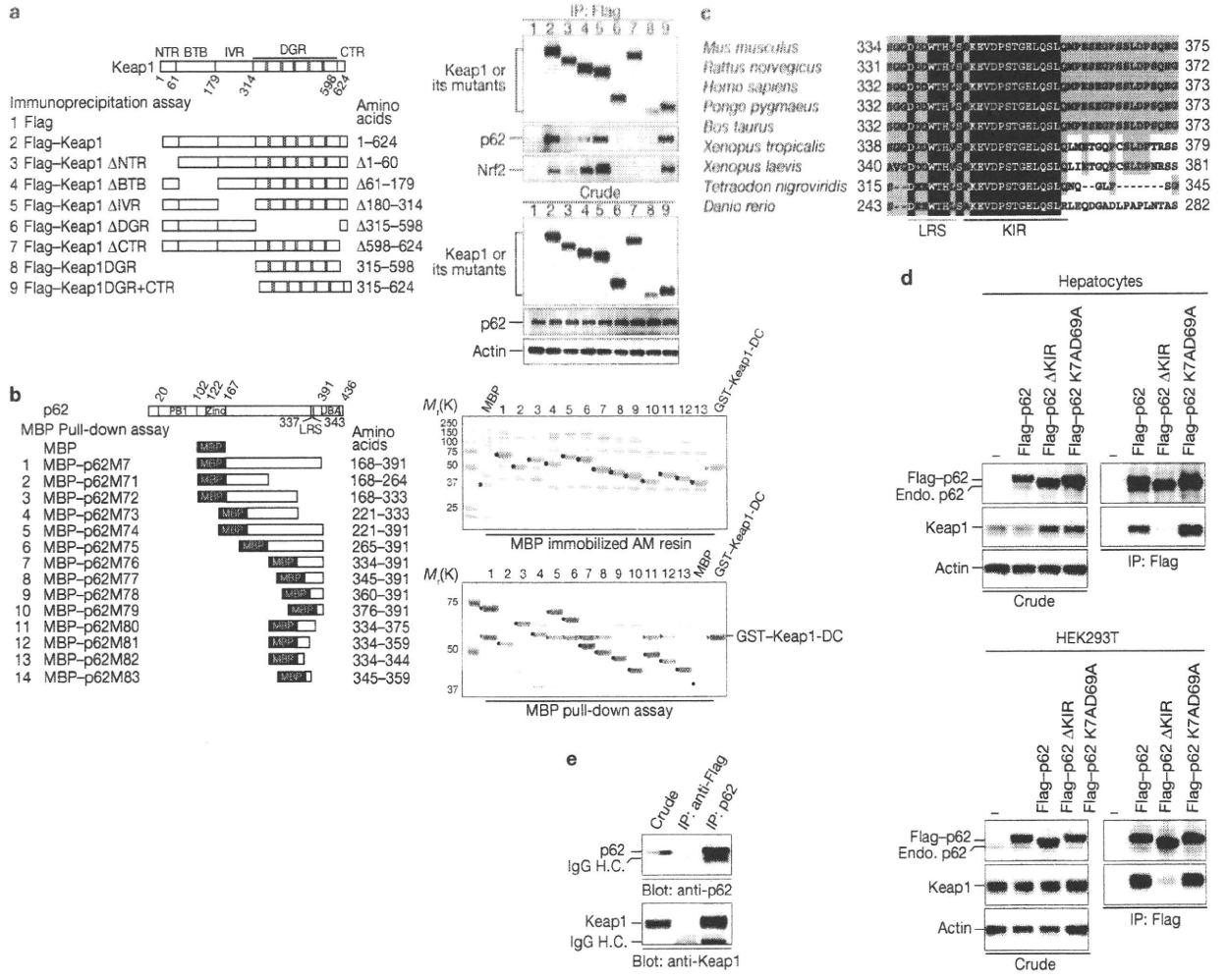

Figure 1 Interaction between Keap1 and p62. (**a**) Diagrams of the deletion–mutation constructs of Keap1 (left) and the corresponding immunoprecipitation assays (right). Each Flag-tagged mouse Keap1 and mutant was expressed in HEK293T cells. At 22 h after transfection, lysates were prepared and immunoprecipitated with anti-Flag antibody. The resulting immunoprecipitates were subjected to SDS–PAGE and analysed by immunoblotting with anti-Flag, anti-p62, anti-Nrf2 and anti-actin antibodies. Data are representative of three individual experiments. (**b**) Diagrams of the deletion–mutation constructs of p62 (left) and the corresponding input (upper right) and pull-down assay (lower right). The MBP-tagged mouse p62 deletion mutants conjugated to amylose (AM) resins were incubated with purified GST-tagged mouse Keap1-DC. The pulled-down complexes with the MBP–p62 mutants were subjected to SDS–PAGE and revealed by staining with Coomassie brilliant blue. The bands corresponding to MBP–p62 and its mutants are indicated by black dots. Red arrowheads indicate the band corresponding to GST–Keap1-DC. For details of construct 14 see Supplementary Information, Fig. S3. (**c**) Alignment of the Keap1-interacting regions (KIR; red line) and the LC3-recognition sequences (LRS; green line) of p62 homologues in various species. Black and grey boxes indicate identical amino acid residues with complete and partial conservation, respectively. (**d**) Immunoprecipitation assays. Flag-tagged p62, KIR-deleted p62 (p62 ΔKIR) and a p62 mutant defective in oligomerization (p62 K7AD69A) were expressed in primary mouse hepatocytes by the adenovirus system (left) or in HEK293T cells by transfection (right). Cell lysates were immunoprecipitated with anti-Flag antibody. The resulting immunoprecipitates were subjected to SDS–PAGE and analysed by immunoblotting with anti-p62 and anti-Keap1 antibodies. The bands corresponding to Flag–p62, endogenous p62, Keap1 and actin are indicated. The data shown are representative of three separate experiments. (**e**) Interaction of endogenous p62 with Keap1. Lysates prepared from the human hepatocellular carcinoma cell line Huh-1 were immunoprecipitated with anti-p62 antibody or anti-Flag antibody (negative control) followed by immunoblotting with antibodies against p62 and Keap1. The bands corresponding to endogenous p62, Keap1 and IgG heavy chain (IgG H.C.) are indicated. The data shown are representative of three separate experiments. Uncropped images of blots are shown in Supplementary Information, Fig. S11.

(kelch-like ECH-associated protein 1) is an adaptor of the ubiquitin ligase complex[24–27]. Exposure to electrophiles, reactive oxygen species and nitric oxide instigates the modification of the cysteine residues of Keap1, leading to its inactivation[28–30]. As a result, Nrf2 becomes stabilized and translocates to the nucleus to induce the transcription of numerous cytoprotective genes through its heterodimerization with small Maf proteins[31–33] (see Supplementary Information, Fig. S10). In this study we found that p62 acts to stabilize Nrf2 in autophagy-deficient mouse livers and subsequently induces the expression of various cytoprotective enzymes. This sustained activation of Nrf2 seems to be a major cause of toxicity in autophagy-impaired livers.

RESULTS

Identification of Keap1 as a p62-interacting protein

Previous genetic studies on the autophagy-essential protein Atg7 in the mouse showed that loss of autophagy caused a marked accumulation

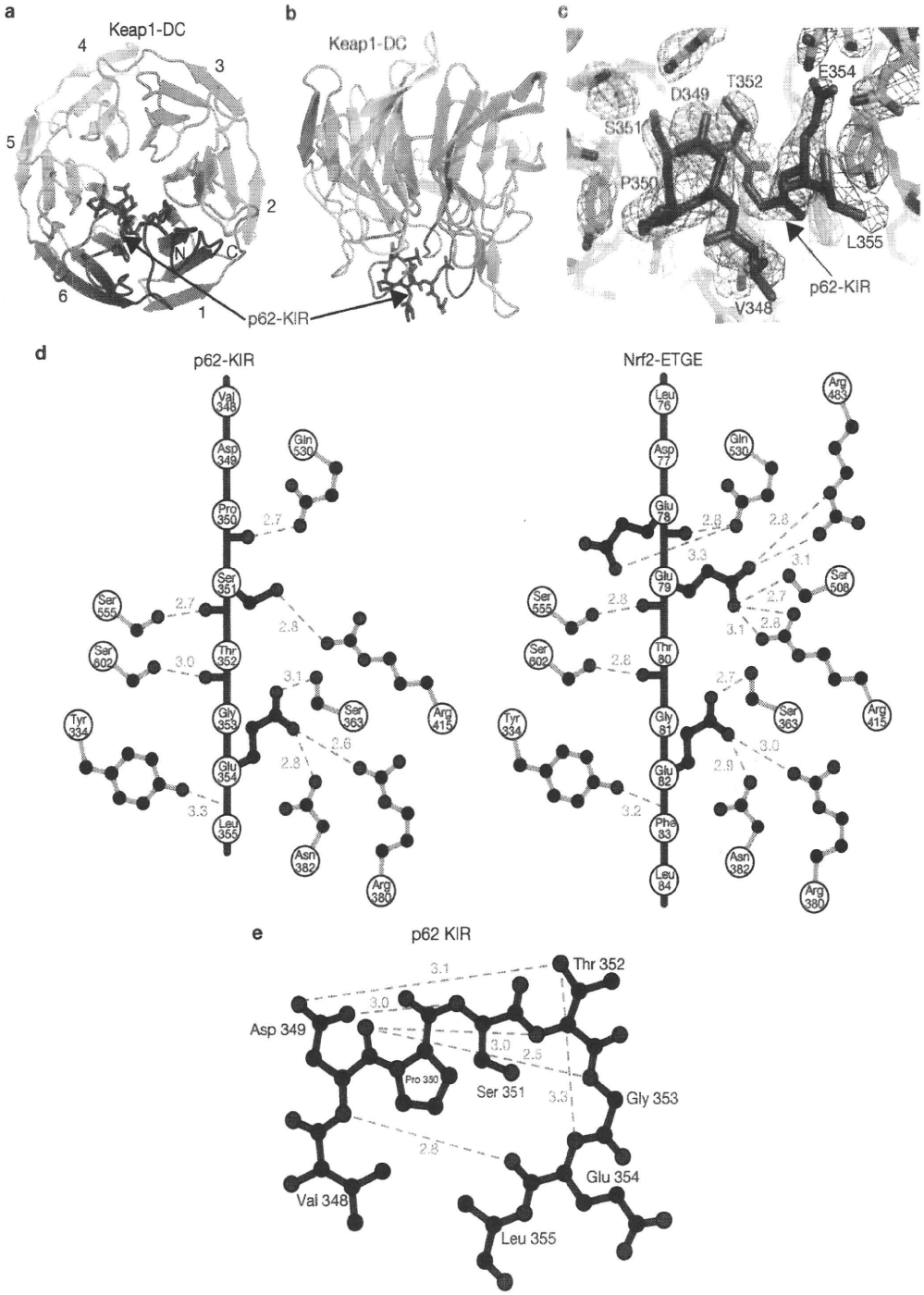

Figure 2 Crystal structure of Keap1-DC in complex with p62-KIR. (**a**, **b**) Bottom view (**a**) and side view (**b**) of the complex structure. The ribbon model represents Keap1-DC and the stick model shows p62-KIR. Each β-propeller blade is numbered from 1 to 6. (**c**) The simulated-annealing $F_o - F_c$ omit map is contoured at 3 σ. p62-KIR (pink) was omitted from the calculation. The electron density of the peptide-bound region V348 to L355 of p62-KIR was unambiguously visible. (**d**) Intermolecular hydrogen bonds of Keap1-DC in complex with p62-KIR (left; PDB ID 3ADE) and in complex with the Nrf2-ETGE region (right; PDB ID 1x2r). (**e**) Intra-peptide hydrogen bonds of p62-KIR in the Keap1-DC complex. Hydrogen bonds (green broken lines) and their distances (Å) are displayed in **d** and **e**.

of p62 along with robust induction of antioxidant proteins, including NAD(P)H dehydrogenase quinone 1 (Nqo1) and glutathione *S*-transferase (GST)[16]. A battery of such detoxifying and antioxidant genes is regulated by the transcription factor Nrf2, which is activated by oxidative and electrophilic stresses[31,32] (see Supplementary Information, Fig. S10). A prominent accumulation of Nrf2 in the nucleus was observed in livers deficient in Atg7, but this was ameliorated by the additional loss of p62 (ref. 16). We therefore postulated that in autophagy-deficient livers, oxidative stresses occur in a p62-dependent manner. However, treatment of *Atg7*-deficient hepatocytes with the antioxidant reagent *N*-acetylcysteine did not affect the nuclear accumulation of Nrf2 or the high-level expression of antioxidant enzymes (Supplementary

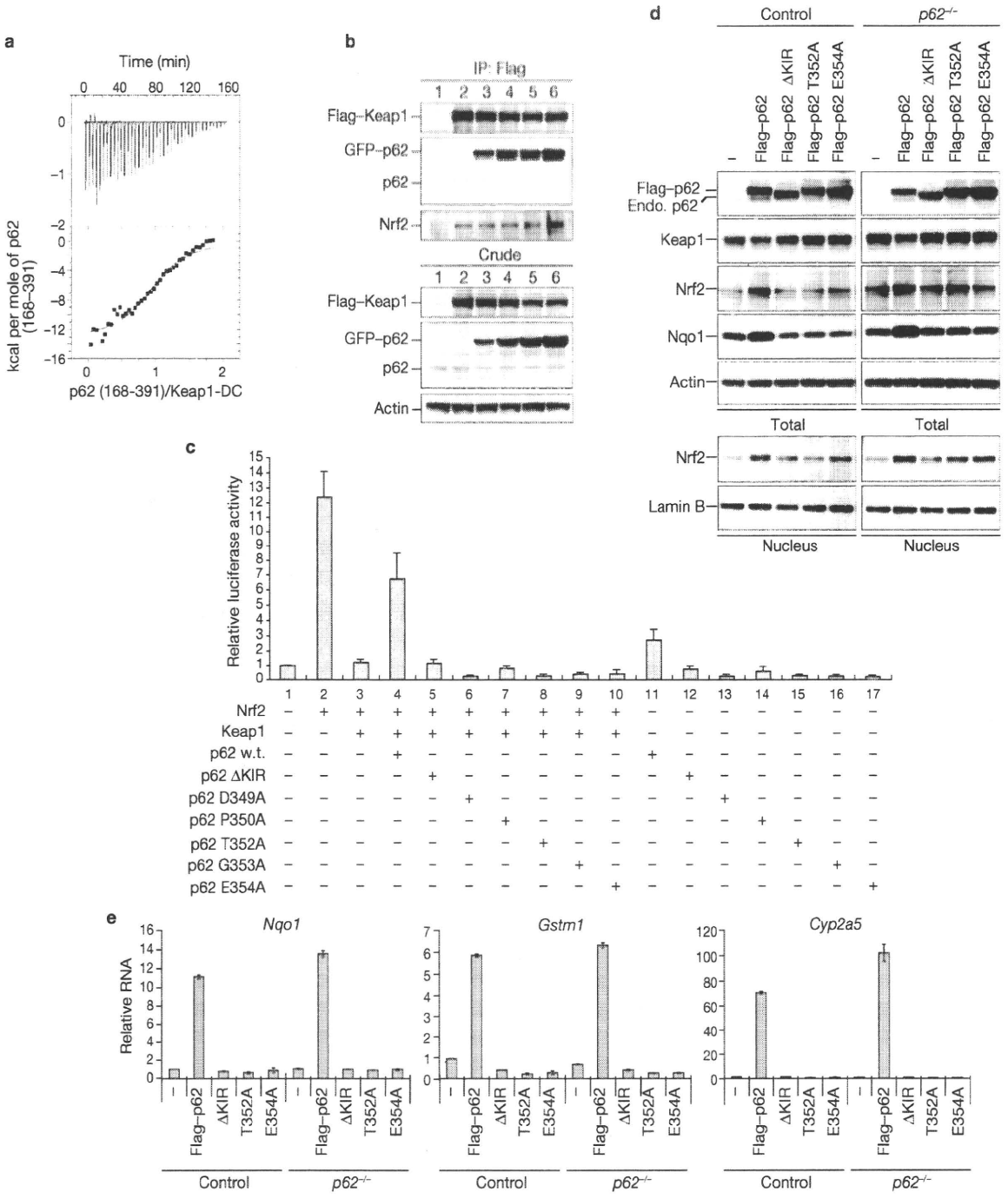

Figure 3 Competitive inhibition of the Nrf2–Keap1 pathway by p62. (**a**) A representative ITC profile of the titration of Keap1-DC with p62M7 (residues 168–391). The upper panel shows the raw ITC thermograms and the lower panel shows the fitted binding isotherms. (**b**) Immunoprecipitation assays. Flag-tagged Keap1 was co-expressed with increasing concentrations of green fluorescent protein (GFP)–p62 (lanes 3–6) in HEK293T cells. Cell lysates were immunoprecipitated with anti-Flag antibody. The resulting immunoprecipitates were subjected to SDS–PAGE and analysed by immunoblotting with anti-Flag, anti-p62 and anti-Nrf2 antibodies. The bands corresponding to Flag–Keap1, endogenous p62, Nrf2 and actin are indicated. Data are representative of three independent experiments. (**c**) The competitive p62 activity against Keap1 was measured by luciferase assay. The expression plasmids for Nrf2, Keap1 and p62 wild-type (w.t.) or its mutants were transfected into Hepa1 cells along with pNqo1-ARE reporter plasmid and pRL-TK as an internal control. At 36 h after transfection, the luciferase activity was measured in accordance with the instructions provided by the manufacturer. Assays were performed twice in triplicate. Data are means and s.d. for six determinations. (**d**) Immunoblot analysis. Flag-tagged p62 and its mutants defective in interacting with Keap1 were overproduced in wild-type and *p62*$^{-/-}$ primary mouse hepatocytes by the adenovirus system. At 48 h after infection, total cell lysates and nuclear fractions were prepared and subjected to immunoblot analysis with the antibodies specified. The bands corresponding to Flag–p62, endogenous p62, Keap1, Nrf2, Nqo1, actin and Lamin B are shown. Data are representative of three independent experiments. Uncropped images of blots are shown in Supplementary Information, Fig. S11. (**e**) Quantification of mRNA levels of the detoxification enzymes Nqo1, Gstm1 and Cyp2a5 in hepatocytes overexpressing Flag–p62 and its mutants. Total RNAs were prepared from non-infected or infected hepatocytes and reverse transcribed into their respective cDNAs, which were used as templates in real-time PCR analysis. Values were normalized to the amount of each mRNA in the non-infected hepatocytes. The experiments were performed three times. Data are means ± s.d. for three experiments.

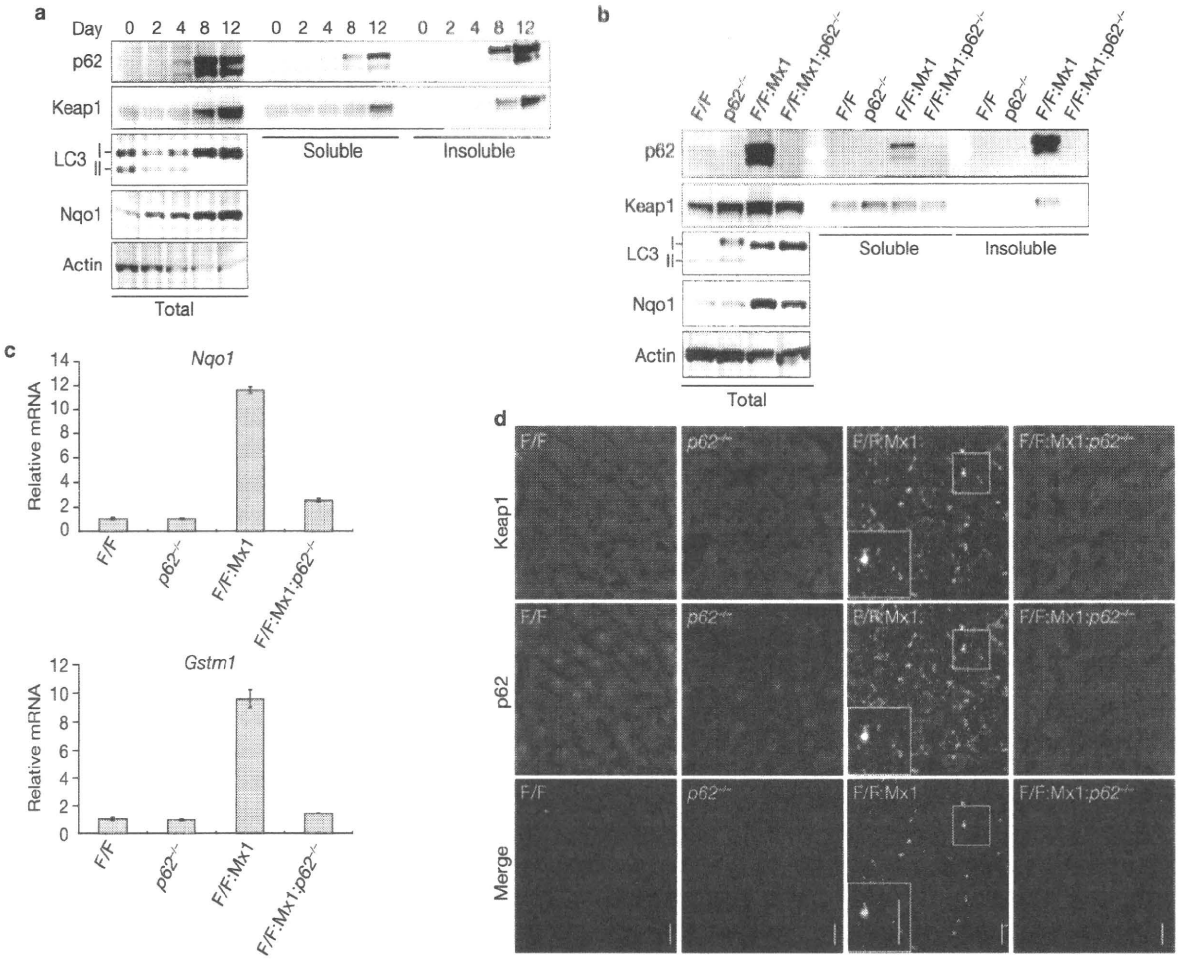

Figure 4 Formation of p62-positive and Keap1-positive inclusions in autophagy-deficient hepatocytes. (**a**) Insolubilization of Keap1 in *Atg7*-deficient hepatocytes. Liver homogenates from *Atg7*$^{F/F}$:Mx1 mice on various days after injection of poly(I)•poly(C) were separated into detergent-soluble and detergent-insoluble fractions with 0.5% Triton X-100. Each fraction was subjected to SDS–PAGE and analysed by immunoblotting with the indicated antibodies. The data displayed are representative of three separate experiments. (**b**) Immunoblot analysis of *Atg7*-deficient (*Atg7*$^{F/F}$:Mx1; *Atg7*$^{F/F}$ shown here as F/F) and *Atg7 p62*-deficient (*Atg7*$^{F/F}$:Mx1:*p62*$^{-/-}$) livers. Liver homogenates from mice of the stated genotypes at 12 days after injection of poly(I)•poly(C) were separated into detergent-soluble and detergent-insoluble fractions. Each fraction was subjected to SDS–PAGE and analysed by immunoblotting with the indicated antibodies. *Atg7*$^{F/F}$ mice[2] in which Atg7 is efficiently expressed at a level similar to that in the wild-type mice were used as control. Data shown are representative of three separate experiments. Uncropped images of blots are shown in Supplementary Information, Fig. S11. (**c**) Quantitative real-time PCR analyses of Nqo1 and Gstm1 in mouse livers. Total RNAs were prepared from livers of the indicated genotypes at 12 days after injection of poly(I)•poly(C). Values were normalized to the amount of mRNA in *Atg7*$^{F/F}$ liver. Data are means ± s.d. for three experiments. (**d**) Immunofluorescence analysis of the cellular localization of p62 and Keap1. Liver sections from mice of the indicated genotypes at 28 days after injection of poly(I)•poly(C) were immunostained with anti-Keap1 (top) and anti-p62 (middle) antibodies. Bottom: merged images of Keap1 (green) and p62 (red). Each inset in the *Atg7*-deficient liver panels is a magnified image of the boxed region. Scale bars, 20 μm.

Information, Fig. S1), suggesting the existence of p62-dependent regulation of Nrf2.

To explore cellular regulation by p62, we used a proteomic approach[34] to screen for proteins that interact with p62, by using HEK293T cells expressing tagged p62 protein. Keap1 was identified as a p62-interacting protein (data not shown). In an independent experiment with RL34 cells expressing tagged Keap1 protein, we isolated p62 as a Keap1-associating protein (data not shown). Keap1 is a substrate adaptor protein for Cullin-3-type ubiquitin E3 ligase. Keap1 possesses four domains: the Broad complex, Tramtrack, and Bric-a-Brac (BTB, amino-acid residues 61–179); the intervening region (IVR, residues 180–314); the double glycine repeat or kelch repeat (DGR, residues 315–598); and the carboxy-terminal region (CTR, residues 599–624)[24–27] (Fig. 1a). The DGR and CTR domains are collectively called the DC domain. The BTB domain serves to dimerize Keap1, enabling ubiquitin conjugation onto specific lysine residues located within the Neh2 domain of Nrf2 (refs 35, 36). The IVR domain interacts with Cullin 3 to promote Nrf2 ubiquitylation[26], whereas the DC domain physically interacts with the Neh2 domain of Nrf2 (refs 36 37). To specify the regions of Keap1 essential for its interaction with p62, we performed an immunoprecipitation assay. Whereas Keap1 C-terminal deletion mutants (ΔDGR and ΔCTR) did not interact with either endogenous p62 or Nrf2, Keap1 amino-terminal deletion mutants (ΔNTR, ΔBTB and ΔIVR) interacted with both endogenous p62 and Nrf2, although with weaker affinities than wild-type Keap1 (Fig. 1a). The Keap1-DC domain, but not the DGR domain, bound to both p62 and Nrf2 (Fig. 1a). The CTR domain contributes to the structural fold of Keap1-DC, which is required for interaction with Nrf2 (ref. 38). These results therefore suggest that the six-bladed β-propeller structure of Keap1 is essential for its molecular recognition of p62, as is the case for Nrf2.

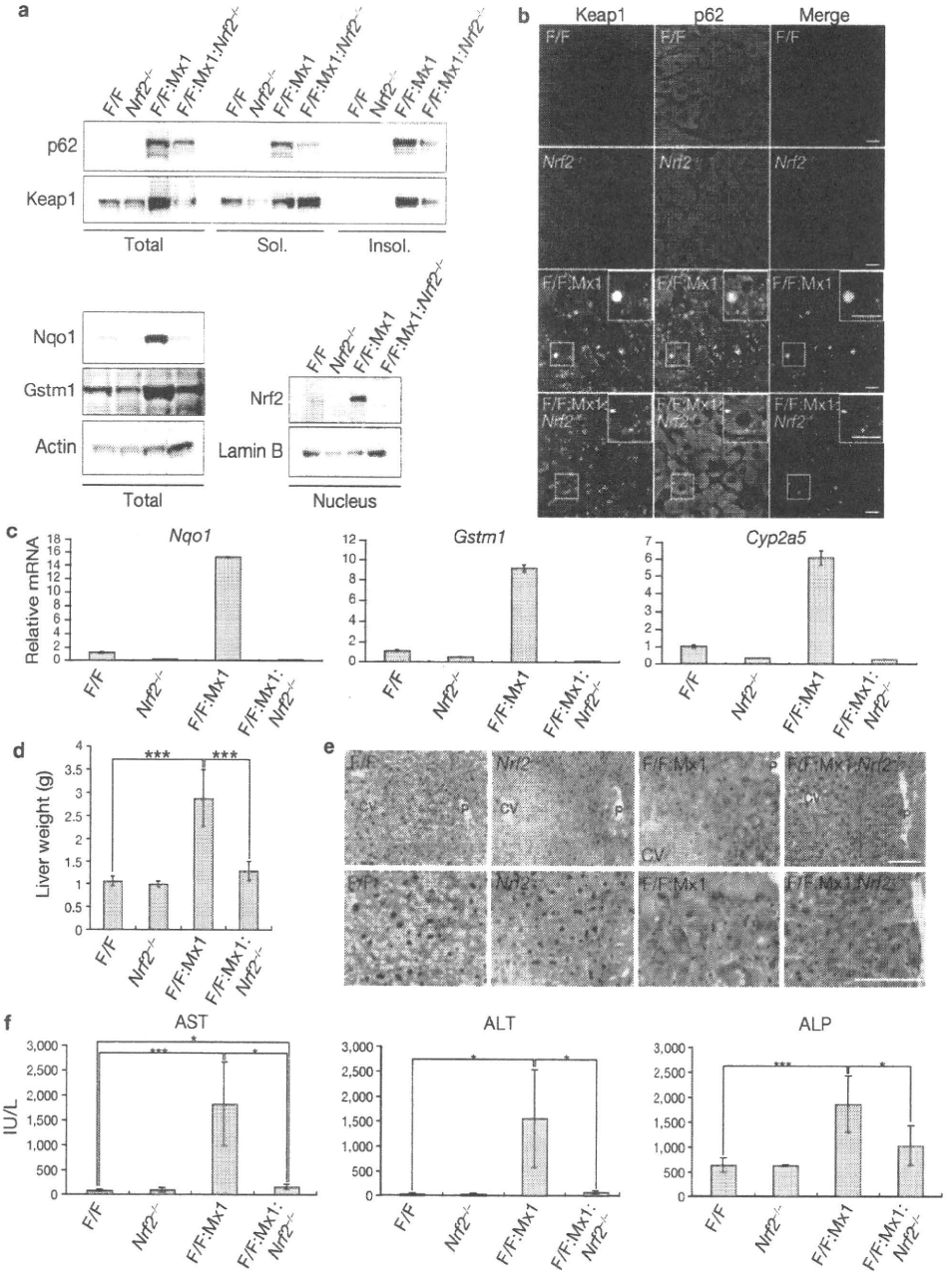

Figure 5 Amelioration of liver dysfunction in autophagy-deficient mice by the additional loss of *Nrf2*. (**a**) Immunoblotting of *Atg7*-deficient (*Atg7*$^{F/F}$:Mx1; *Atg7*$^{F/F}$ shown here as F/F) and *Atg7 Nrf2*-deficient (*Atg7*$^{F/F}$:Mx1:*Nrf2*$^{-/-}$) livers. Liver homogenates from mice of the assigned genotypes at 28 days after injection of poly(I)•poly(C) were separated into detergent-soluble and detergent-insoluble fractions. Total, soluble and insoluble fractions were subjected to SDS–PAGE and analysed by immunoblotting with the indicated antibodies (top section). Total lysates were subjected to SDS–PAGE and analysed by immunoblotting with antibodies against Nqo1, Gstm1 and actin (bottom left section). Nuclear fractions were prepared from the livers of the indicated genotypes at 28 days after injection of poly(I)•poly(C), subjected to SDS–PAGE and analysed by immunoblotting with antibodies against Nrf2 and Lamin B (as control) (bottom right section). Data were obtained from three independent experiments. Uncropped images of blots are shown in Supplementary Information, Fig. S11. (**b**) Immunofluorescence analysis of the cellular localization of p62 and Keap1. Liver sections from mice of the indicated genotypes at 28 days after injection of poly(I)•poly(C) were immunostained with anti-Keap1 (left) and anti-p62 (middle) antibodies. Right: merged images of Keap1 (green) and p62 (red). Each inset in the *Atg7*-deficient and *Atg7 Nrf2*-deficient liver panels is a magnified image of the boxed region. Scale bars, 20 μm. (**c**) Quantitative real-time PCR analyses of Nqo1, Gstm1 and Cy2a5 in mouse livers. Total RNAs were prepared from livers of the indicated genotypes at 28 days after injection of poly(I)•poly(C). Values were normalized to the amount of mRNA in the *Atg7*$^{F/F}$ liver. Data are means ± s.d. for three experiments. (**d**) Liver weight. The weights of the mouse livers of the different genotypes shown at 28 days after injection of poly(I)•poly(C) were measured. Data are means ± s.d. for five mice from each group. Three asterisks, $P < 0.001$ (Student's *t*-test). (**e**) Histological analysis of the mouse liver of the indicated genotypes. At 28 days after injection of poly(I)•poly(C), the livers were processed for haematoxylin/eosin staining. Higher-magnification views are shown in the bottom panels. CV, central vein; P, portal vein. Scale bars, 100 μm. (**f**) Liver function tests of the mice used in **d**. The serum levels of aspartate aminotransferase (AST), alanine aminotransferase (ALT) and alkaline phosphatase (ALP) were measured. (IU/L, international unit per liter). Data are means ± s.d. for seven mice from each group. Asterisk, $P < 0.05$; three asterisks, $P < 0.001$.